Optimal design and operation of thermal energy storage systems in micro-cogeneration plants

Pérez-Iribarren E.[(a*)], González-Pino I.[(a)], Azkorra-Larrinaga Z.[(a)], Gómez-Arriarán I[(b)].

(a) ENEDI Research Group, Department of Thermal Engineering, Faculty of Engineering of Bilbao, University of the Basque Country UPV/EHU, Plaza Ingeniero Torres Quevedo 1, 48013 Bilbao, Spain.

(b) ENEDI Research Group, Department of Thermal Engineering, Faculty of Engineering of Gipuzkoa, University of the Basque Country UPV/EHU, Europa Plaza 1, 20018 Donostia, Spain.

[*]Corresponding author: Tel.: +34946017346. E-mail: estibaliz.perezi@ehu.eus

ABSTRACT

The implementation of micro-cogeneration plants in residential buildings requires a technical and economic viability study. This analysis depends greatly on the regulatory framework controlling this kind of installations, which is characterized by its variability and great uncertainty. Viability is also closely related to the sizing of devices and their integration within the plant, as well as to its global operation. Although different methods are used for sizing micro-cogeneration installations, there is no methodology to determine the optimal capacity of the thermal energy storage and the auxiliary generation system in the design phase. Since the optimal strategy of the whole plant is not taken into account in this project phase, the installation is usually oversized, decreasing the efficiency of the plant and increasing the overall cost. The aim of this paper is to analyze the viability study of micro-cogeneration systems with integrated thermal energy storage and determine the influence of this on the final results. Furthermore, a mathematical linear programming-based model is proposed, where the optimal behavior of the different devices is predicted in the design phase in order to determine the optimal sizing of both the tank and the auxiliary boiler. The developed model can be a useful tool in viability analysis and can easily be reproduced by engineers and researchers. In conclusion, the optimal integration and sizing of the thermal energy storage considerably improve the thermodynamic, economic and environmental results.

Keywords: micro-cogeneration; linear optimization; hybrid systems; economic analysis; marginal costs.

Abbreviations

CTE	Technical Building Code
CCHP	Combined Cooling, Heat and Power
CHP	Combined Heat and Power
DHW	domestic hot water
EA	Evolutive Algorithm
GA	Genetic Algorithm
GHG	greenhouse gas
HHV	High Heating Value
ICE	Internal Combustion Engine
IEA	International Energy Agency
LHV	Low Heating Value
MILP	Mixed Integer Linear Programming
MINLP	Mixed Integer Non-Linear Programming
TES	Thermal Energy Storage
TUR	last resource tariff

Nomenclature

bin	binary
C	cost (€)
CHAR	charging binary variable
CRF	capital recovery factor (-)
cw	specific heat of water (kJ/(kg·K))
d	day
D/H	diameter/height ratio of thermal storage (-)
DISCH	discharging binary variable
E	electric energy (kWh)
$\dot{E}$	electric power (kW)
F	fuel energy (kWh)
$\dot{F}$	fuel power (kW)
h	hour
i	annual interest rate (%)
ICE	internal combustion engine binary variable
Inv	total investment (€)
M	constant of big M method
Min	minimize
n	lifetime (year)
NPV	net present value (€)
NS	annual net savings (€)
NTD	number of times that each day is repeated (day/month)
PL	partial load (per unit) PSU penalty to starting up (per unit)
PES	primary energy saving (% or kWh)
Q	thermal energy (kWh)
$\dot{Q}$	thermal power (kW)
r	ratio of discount (%)

REE	equivalent electric efficiency (%)
$RefE_\eta$	harmonised efficiency reference value for separate production of electricity (%)
$RefH_\eta$	harmonised efficiency reference value for separate production of heat (%)
start-up	function of the operation mode of engine
t	period of time (h)
T	temperature (°C)
V	volume (l)
V2V	two-way valve
x	variable

Greek symbols

γ	auxiliary variable (-)
δ	auxiliary variable (-)
η	efficiency (%)
ρ	density (kg/m³)

Subscripts

CAP	capacity of thermal storage
CB	condensing boiler
CHAR	charging process
CHP	cogeneration system
DEM	demand
DHW	domestic hot water demand
DISCH	discharging process
E	electricity
EPUR	purchased electricity
ESOLD	sold electricity
F	fuel
HEAT	heating demand
ICE	internal combustion engine
ICE,U	useful product of the internal combustion engine
INV	investment
k	technology
LOSS	losses
MIN	minimum
NOM	nominal value
O&M	operation and maintenance
PUR	purchase
Q	heat
r	return STO stored thermal energy
TES	thermal energy storage
TOT	total
VM	variable maintenance prices

1.   Introduction

The technical, economic and environmental feasibility of micro-cogeneration plants –according to the cogeneration directive published in 2004 [1], cogeneration units with electric power below 50 kW$_e$– in the residential sector is intimately tied to the correct sizing of micro-CHP and thermal energy storage systems, as well as to operation factors such as the operation hours of the micro-CHP unit or the dissipation of residual heat. Furthermore, the variability of thermal demands in the building sector, the high volatility of market prices and the great uncertainty in the regulatory framework of cogeneration, all imply a difficulty in operating, sizing and selecting the equipment that integrates a micro-CHP plant. Therefore, viability depends on the capacity and operational strategy of the different devices of the plant, so optimization methods are indispensable for exploiting the plant's overall potential. The optimization of thermal installations becomes more complex due to the fact that some legal or operational constraints do not have the same hourly basis, which implies that the optimal annual operation does not correspond to the sum of the optimal hourly results. In the case of thermal installations, operational constraints have an hourly basis, whereas many of the legal restrictions of cogeneration are applied on an annual basis (minimum energy efficiency required, minimum primary energy saving, etc). If, in addition, the cogeneration plant integrates a TES system, the complexity of the optimization increases considerably with the additional variable of thermal storage level. This fact implies that the optimal operation of a certain instant depends totally on the operation of the plant in the previous one. This implies that it is not possible to study separately each of the hours of the temporary horizon considered, thus substantially increasing the number of possible solutions [2].

The number of decision variables changes depending on the phase considered in the optimization problem of thermal installations (synthesis, design or operation). The synthesis of the system implies the selection of the technologies that constitute the overall system, besides the existing interconnections between them. For this, a superstructure considering the technologies susceptible to be installed and the possible interconnections between them is defined. Once the technology installed is known, the optimization of the design focuses on the technology sizing (nominal power or number of devices installed), for which it is necessary to determine technical characteristics and cost of investment (for economic optimization) or carbon dioxide emissions generated by the manufacturing (for environmental optimization). Finally, the operation is optimized according to the primary energy consumption, the cost, or the environmental impact generated by the plant's operation.

In order to approach this type of problems, several methods have been proposed over the last few decades; from heuristics (genetic algorithms, swarm of particles, ant colony algorithms, tabu-search, fuzzy logic, dynamic programming and Lagrangian relaxation methods [3]), to mathematical programming (Mixed Integer Linear Programming: MILP or Mixed Integer Non-Linear Programming: MINLP [4]). MILP solvers –which are based on solid math foundations and efficient codes for the treatment of integer and binary variables– have improved considerably over the last few years; the conversion of original MINLP problems into MILP –by means of approximation of the non-linear constraints into linear ones– being a very commonly used method [5].

Heuristic methods are useful for solving large-size and/or non-linearizable problems. Compared to MILP, they present the advantage of being very flexible and more efficient for big problems, as well as being able to use non-linear constraints (models closer to real operation) and to be applied to very complex problems [6]. Nevertheless, they also have disadvantages, such as: a) since heuristic algorithms can get trapped in a local optimum of the solution space, solutions provided by heuristic methods can be near to a local optimal solution, whereas MILP returns a global optimal solution; b) unlike MILP, in which the procedure is concise and independent from particularities of the problem, the calculation procedure depends on the initial problem and its structure, so that technologies applied to its resolution are specific to the problem in question; c) they depend on the structure of the problem and cannot adapt to modifications in the initial problem, whereas MILP allows this to be optimized.

Heuristic methods have been widely used in the optimization of CHP and CCHP systems [7], principally the most sophisticated ones, such as evolutionary algorithms (EA) or genetic algorithms (GA). These methods are used for the optimization of the operation as an internal routine inside an iterative optimization sizing problem, where installation design and configuration have to be previously defined [8]. Thus, an integrated treatment of all the levels of optimization (operation, design and synthesis) is not considered.

Even though MILP presents greater mathematical complexity in its formulation – as well as in the definition of linear models –, the aforementioned advantages have stimulated its use. In the last few years, the use of MILP has been encouraged for the optimization of the operation, design and synthesis of CHP[9] and CCHP plants [10,11], due to the possibility of solving large scale problems that it offers, with multiple variables and constraints, by means of a "horizontal algorithm" where the variables of operarion, design and synthesis are treated in a similar way and at the same level [12]. Regarding TES integration in CHP and CCHP plants, MILP has been used to optimize the operation of previously sized plants [2, 9-11] or the operation, sizing and synthesis of plants without the TES

system [2, 9-11]. However, the feasibility of CHP plants –which commonly integrate TES systems–not only depends on the operation strategy of devices, but also on their correct sizing.

Despite the fact that different methods are used by engineers and researchers, there is no methodology that allows the optimal strategy, sizing and selection of the principal devices which compose a micro-CHP plant (micro-CHP unit, thermal energy storage and auxiliary thermal generator) to be determined. In this paper, a MILP model for simultaneously optimizing the operation and sizing for residential micro-CHP plants is carried out, where the variability in thermal and electrical demands and the uncertainty in the market prices and in the regulation of energy efficiency in buildings are considered.

According to the above, in this paper, the following aims are pursued: a) the development of an integer linear programming-based model that allows the sizing and operation of the principal equipment in a micro-CHP plant with thermal storage to be optimized; b) the analysis of the integration of the TES systems in micro-CHP plants and c) the determination of the configuration and capacity which optimizes the sizing and operation technically, economically and environmentally, as well as the advantages of the correct TES sizing.

2. Design criteria in micro-CHP plants

2.1. Design and choice of the micro-CHP unit

Amongst the design criteria used for the selection of a micro-cogeneration unit, two can be highlighted: a) based on heat demand or b) based on electricity demand. In the case of the selection based on electricity demand, this is subject to a great uncertainty due to the evolution of the market prices of electricity (which depends on the normative framework), and to an increase in the dissipated heat, which diminishes the primary energy saving (PES) and the global efficiency of the plant [13].

For this reason, the method based on heat demand is more commonly used in the design of devices in micro-CHP plants, for which the objective is to maximize the cogenerated thermal power. This implies knowing the hourly thermal demand required by the end-users, which includes heating and DHW. From this information, the monotonic demand curve is determined, which represents the cumulative annual demand. In order to define this curve, it is necessary to calculate the number of hours the micro-CHP will operate for each demand point, the minimum number of operation hours corresponding to the maximum thermal power (peak power) and 100% of the operation hours to the minimum thermal power.

The thermal capacity of a micro-cogeneration unit is determined by means of the rectangle with the largest area that can be inscribed under the monotonic curve (maximum rectangle method), which is represented by the blue rectangle in Fig. 1. In agreement with the criteria used by manufacturers and installers, it is recommended that the power of the micro-CHP unit does not surpass 20% of the maximum demand, the lower and upper bounds being 10% (blue line) and 30% (red line), respectively. This is due to the fact that the lower-size device can operate for a greater number of hours continuously, avoiding recurrent on-off cycles which can be harmful to the device and hence considerably reduce its useful life [14].
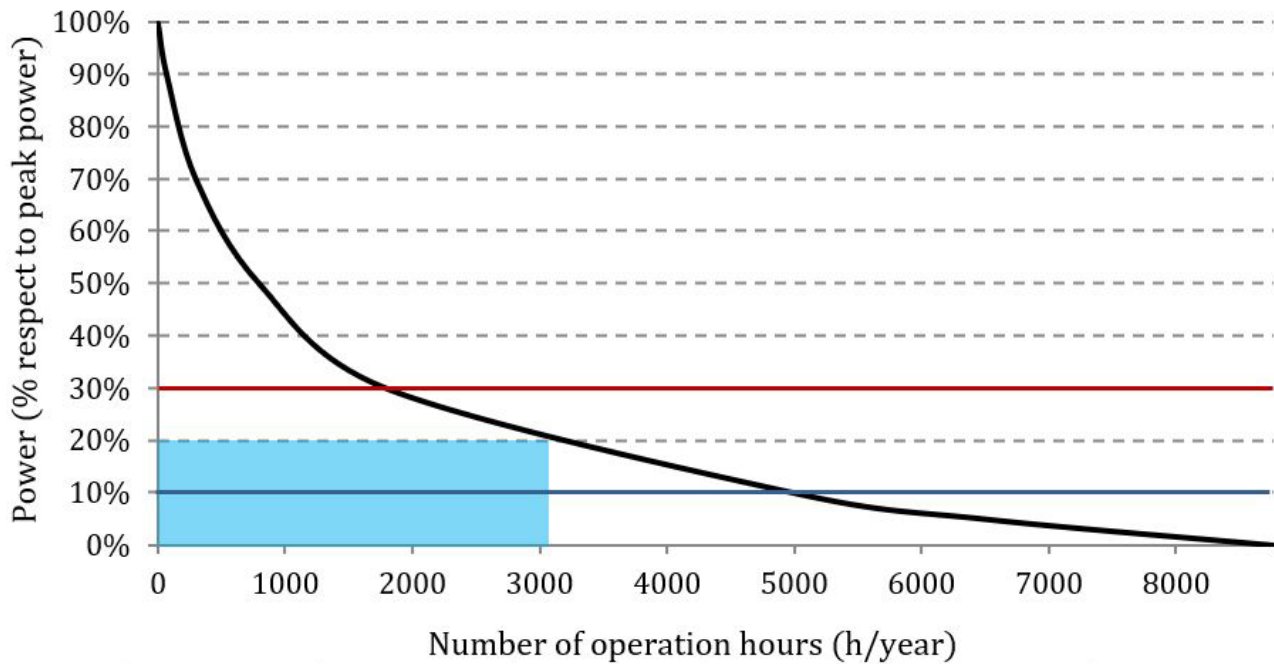
Fig. 1. Monotonic curve of heat demand

The conventional method for sizing a CHP device - based on the maximization of the thermal production - presents the disadvantage that, on numerous occasions, the maximum thermal production requires a high nominal power unit which operates during a low number of hours to be installed. In order to guarantee a more continuous operation of the micro-CHP unit, and consequently to increase its useful life, different solutions shown in Fig. 2 are used [15]:

A. Installation of a buffer tank: this is the most commonly used solution for increasing the annual use of micro-CHP unit. The thermal energy that is not used is stored and discharged later. With this solution, energy resources are used more efficiently, increasing the primary energy saving and the avoided emissions while decreasing the operation cost.

B. Installation of different micro-CHP units in cascade: when different micro-CHP units are installed, one unit will operate a high number of hours to meet the base-load, whereas the peak-load is provided by a unit with a low annual use. This solution implies a higher investment cost and the optimization of the number of units and their operation strategy. In this optimization, the installation of thermal energy storage should also be taken into account.

C. Use of a modular cogeneration unit: some micro-CHP units can modulate between a certain minimum and maximum capacity, enabling modulation to follow the thermal demand. One disadvantage, depending on the micro-CHP technology, is that the overall efficiency at part load can be quite a bit lower. Moreover, this solution usually integrates a thermal energy storage.

D. Decrease of the installed nominal power: despite the annual use of micro-CHP increases, the annual micro-CHP production decreases. Thus, the operational cost may increase and the primary energy saving may diminish.

E. Dissipation of the heat surplus: the unused part of the thermal energy is not stored, it is wasted. Compared with solution A, both the overall efficiency and primary energy saving decrease. Regarding the cost, the investment cost is lower since the TES is not installed; on the contrary, as resources are not efficiently used, the operation cost is greater.
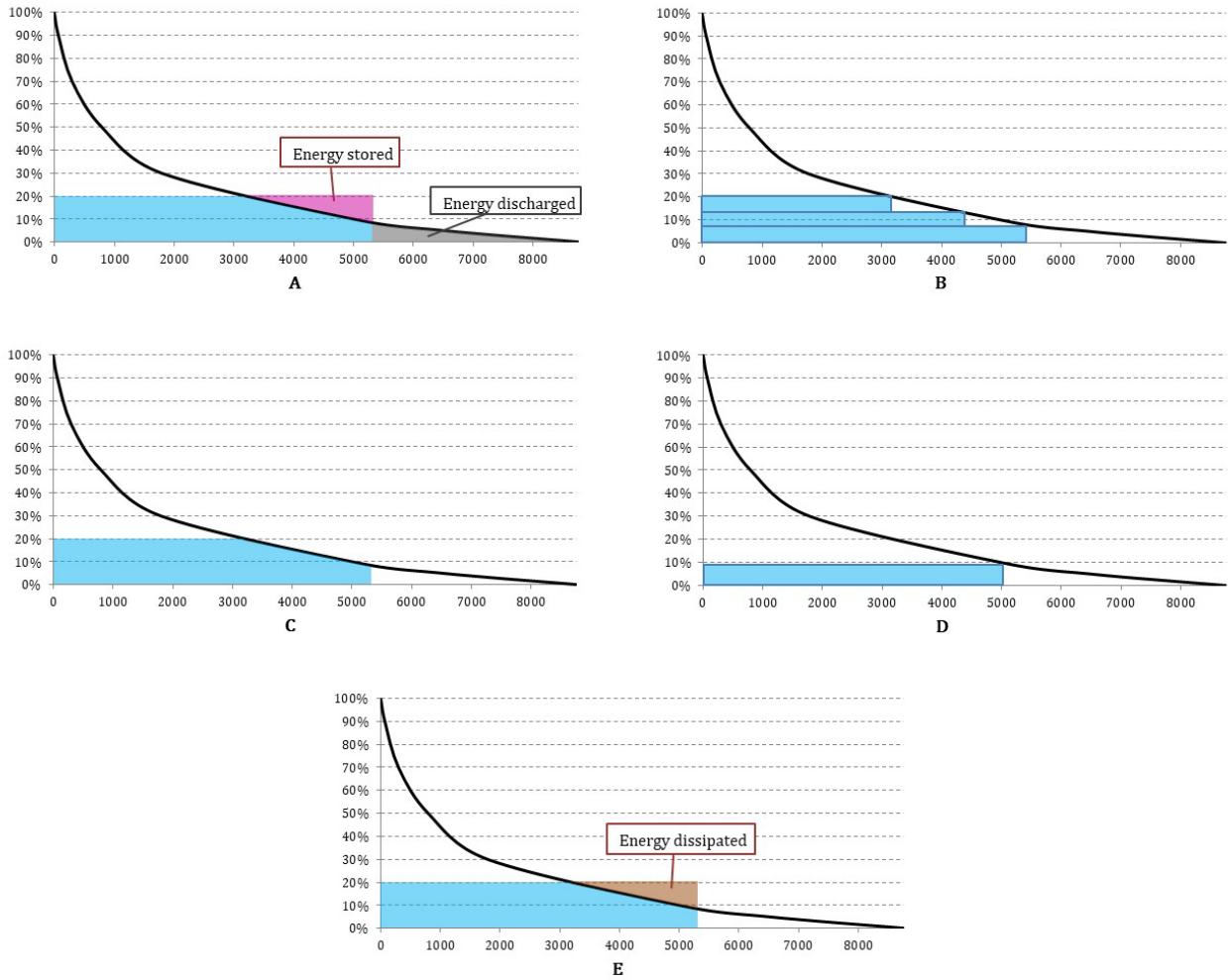
Fig. 2. Solutions for increasing the operation hours of the micro-CHP unit

As mentioned above, solution A presents certain advantages over both solutions D and E. Furthermore, this solution is usually implemented to improve and optimize both B and C. Therefore, solution A is considered in this work.

2.2. Design of thermal energy storage

Installing a TES system is especially interesting when the heating demand has significant periodic variations. In such cases, heat storage allows the dissipated heat to be reduced, as well as the consumption of fuel in conventional boilers and the optimal size of the cogeneration unit. These facts involve an increase in the energy efficiency and a decrease in the annual economic cost of the overall plant [16].

In order to reach the aforementioned aims, a correct sizing of the storage system is necessary. Engineering companies, for instance, use rough methods for sizing inertia tanks, supposing that the minimal volume corresponds to the energy stored during an hour's operation of the micro-cogeneration unit [14].

$$V_{MIN} = \frac{Q_{CHP} \cdot t \cdot 3600}{cw \cdot \rho \cdot \Delta T}$$

Eq. 1

where V_{MIN} is the minimal capacity of the inertia tank in liters, Q_{CHP} is the nominal power of the cogeneration module in kW, t is the storage time in hours, cw is the specific heat in kJ/kg·K, ρ is the density in kg/l, and ΔT is the temperature difference between top and bottom in the tank in K.

However, these rough methods usually lead to an inadequate sizing of the TES, which can imply oversizing and, consequently, an increase in the investment and the required space, greater heat losses and a decrease in the potential primary energy savings of the installation [17].

Apart from this, the effect of the TES in cogeneration systems is non-linear [18], due to the variability of the demand profiles, the characteristics of the equipment, the effects of the charging and discharging processes of the TES and the on-off periods of the thermal systems. This makes the calculation of the optimal size of the TES rather difficult. There are numerous methodologies for sizing the TES, from simple methods to methods with greater mathematical complexity.

Within the methods of lower complexity, it is worth pointing out the iterative optimization strategy (heuristic), which is based on the search of the optimal operation mode, bounding and comparing the most reasonable operation modes of the CHP plant until the optimal solution is reached. This method has been widely used in the last few years for the case of internal combustion engines coupled with TES [19] and its application in simple heat storage systems with two levels of temperature [16], obtaining results as good as those obtained with more sophisticated methods.

Another method of rough sizing is based on annual PES [17]. This simple method is applied to Combined Cooling Heat and Power systems (CCHP), with the aim of estimating their capacity and operation strategy, under the hypothesis that generated electricity is spilt to the grid. This strategy combines different methods of evaluation to find the optimal capacity of the TES that increases the number of operation hours, while maintaining the PES over the minimum threshold. Different cases have been analyzed, obtaining similar results to more complex methods.

The most sophisticated sizing methods use optimization algorithms for the overall design of the installation. These are based on heuristic methods by means of genetic algorithms [20] or on mathematical linear [10, 21] or non-linear [22] models.

2.3. Integration of cogeneration systems and thermal storage in buildings

The installation of micro-CHP systems requires an auxiliary boiler and a TES, where generation devices can be hydraulically integrated in series or parallel [23]. In the series configuration (Fig. 3), the micro-CHP unit is connected to the return pipe; whereas the boiler –which operates as support for the cogeneration unit– is directly connected to the exit of the CHP device. This integration is very useful for simple configurations of heating and DHW and guarantees long periods of operation of the CHP unit.
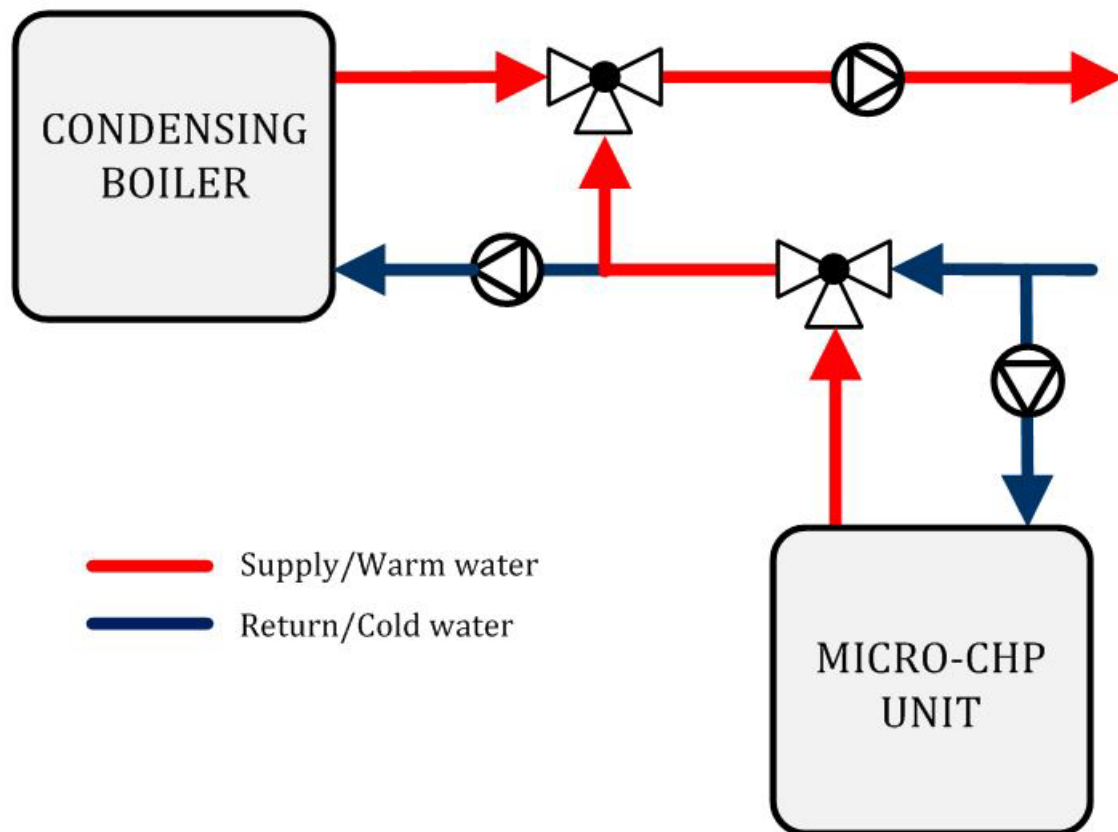

Fig. 3. Series configuration of micro-CHP unit and auxiliary boiler

7

On the other hand, the parallel configuration is the most commonly used in installations of residential buildings and in more complex configurations. When generation systems are integrated in parallel, as represented in Fig. 4, the return water is distributed between the different generation devices and this allows greater efficiencies of the individual devices to be achieved. Regarding the operation of thermal generation units, the control of the plant must be implemented giving priority to the micro-CHP unit over auxiliary systems. This control reduces the on and off cycles of the CHP unit and increases the number of hours that it operates in a continuous way. For these reasons, from here on, this configuration is to be considered.
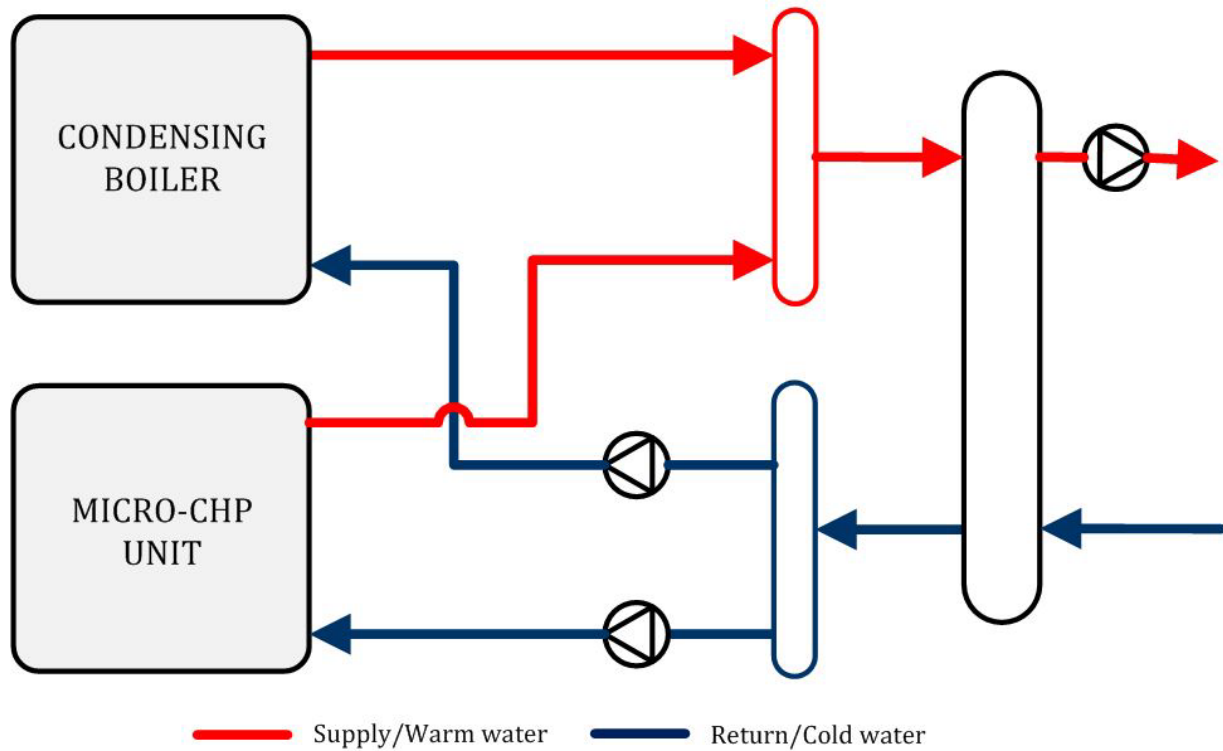
Fig. 4. Parallel configuration of micro-CHP unit and auxiliary boiler

As aforementioned, the integration of the TES has a significant influence on the operation of the installation and its global efficiency; so it is important to analyze the behavior of different configurations. Two possibilities are considered: thermal storage installed in the return or an intermediate accumulation.

In Fig. 5, the hydraulic diagram of the parallel configuration of the generation systems with thermal storage integrated in the return can be observed. In this configuration, if the return temperature is higher than the accumulation temperature, the buffer tank is charged by connecting the return of the radiators to the top of the tank (V2V-1: ON; V2V-2: OFF; V2V-3: OFF) and the bottom of the tank to the inlet of the micro-CHP unit; hence, sending the return water at a lower temperature after storage. When the accumulation temperature reaches a certain value and there is thermal energy demand, the tank is discharged. The discharging is carried out by closing the on-off two-way valve V2V-1 –avoiding the charging of the tank–, and opening the on-off two-way valve V2V-2 that distributes the return-flow from the buffer tank to the micro-CHP unit. Thus, it is possible to supply thermal energy from both the micro-CHP unit and the buffer tank simultaneously (V2V-1: OFF; V2V-2: ON; V2V-3: ON). If the return temperature is lower than the accumulation temperature and the discharging requirements are not fulfilled, the return of the radiators is directly connected to the inlet of the micro-CHP unit (V2V-1: OFF; V2V-2: OFF; V2V-3: ON).
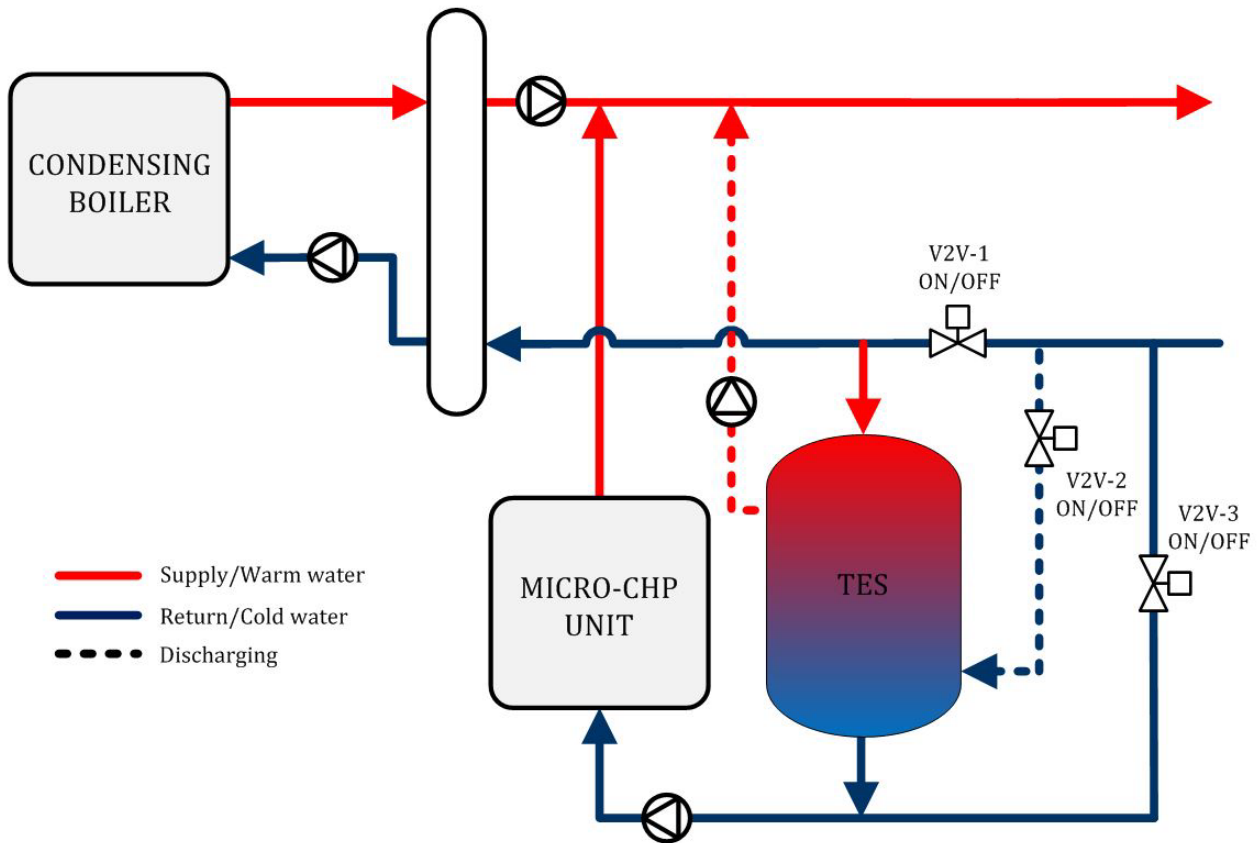
Fig. 5. Parallel configuration of micro-CHP unit and auxiliary boiler, with TES integrated in the return

Thermal storage can also be integrated between the generation systems and the demand. In Fig. 6, the parallel connection of the generation systems with intermediate accumulation is shown. In this case, the micro-CHP unit works by directly charging the tank and discharging to users when thermal energy is demanded. This configuration allows the tank to be charged and discharged at the same time through a 3-way valve, working the tank as a hydraulic compensator. The installation can be controlled, avoiding simultaneous charging and discharging. The advantages and disadvantages of the different configurations of TES integration are analyzed in this paper.
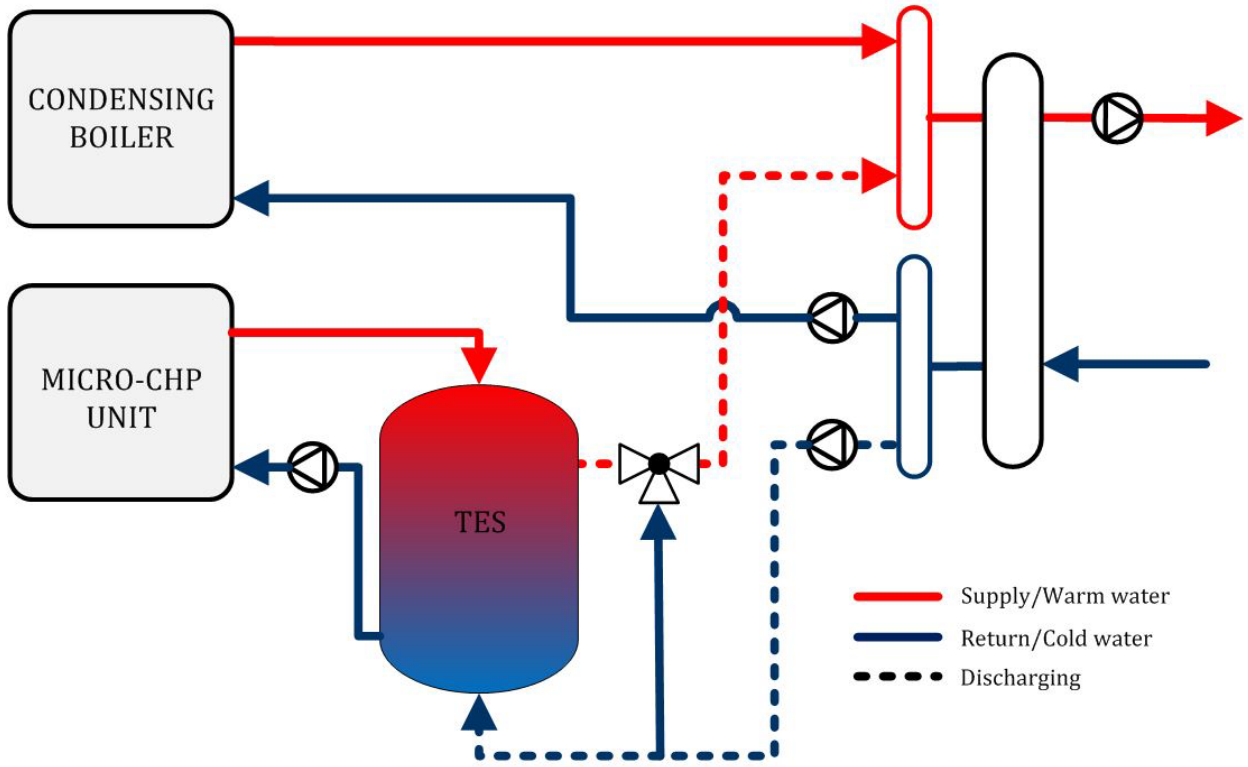
Fig. 6. Parallel configuration of micro-CHP unit and auxiliary boiler, with intermediate integration of TES

3. Design and strategy optimization of micro-CHP plants

The optimization problem of both the sizing and operation of the plant can be solved by means of mathematical linear modeling. In these mathematical models, the global cost of the installation is minimized subject to constraints that represent the configuration of the installation. A feasible design of the installation corresponds to a solution that satisfies all these constraints.

MILP modeling presents the characteristic of including continuous, integer and binary variables. This modeling approach presents important advantages in the design and operation optimization of distributed generation [9, 24]. Since the real behavior of these plants obeys non-linear functions, linear programming requires them to be modeled and linearized. Integer and binary variables allow modeling and decisions to be made about complex situations that take place in this type of plants, where the decision variables of the problem represent units that cannot be divided: start-up and shutdown of devices, number of units to be installed and operative, charging and discharging of tanks, purchase or sale of electricity, etc.

Furthermore, MILP models provide, by means of a relatively simple linear programming model, quantitative and/or qualitative information about the optimal configuration of the plant, which guarantees the minimization of the global cost, while covering the energy needs of the users. MILP algorithms can reach the optimal global solution in problems with multiple variables and restrictions faster than heuristic methods.

The summation form of a standard linear optimization problem consists of minimizing or maximizing a linear objective function:

$$Min\ (Max)\ f(x) = \sum_{j=1}^{n} c_j \cdot x_j \qquad \text{Eq. 2}$$

Subject to linear equality and inequality constraints:

$$\sum_{j=1}^{n} a_{ij} \cdot x_j \leq b_i \quad \text{for } 1 \leq i \leq m \qquad \text{Eq. 3}$$

With non-negative variables:

$$x_j \geq 0 \quad \text{for } 1 \leq j \leq n \qquad\qquad \text{Eq. 4}$$

Within the optimization problem, c_j, a_{ij} and b_i are constant and x_j corresponds to decision variables.

The optimization model can be implemented in linear and integer optimization tools. In this paper, OpenSolver software is chosen, which uses the Open Source CBC (COIN-OR Branch and Cut) linear optimization engine that is implemented as a complement of the Excel VBA [25]. Many times, when optimization codes are applied to real situations, the problem size is large, with multiple decision variables and constraints. The CBC solver allows large-scale MILP models to be solved, obtaining performances and solve-times similar to its commercial equivalents [26]. For that purpose, simplex and Branch and Bound algorithms are used. The CBC solver has gained a reputation in terms of accessibility, quality and reliability, being widely used in research and industrial applications [27, 28]. It has the added advantage of being compatible with other linear programming solvers, such as Gurobi, GAMS or AMPL.

3.1. Selection of representative days

The residential and tertiary sector is characterized by energy demands with great daily and seasonal fluctuations, which are mainly due to climatic conditions and occupational patterns of buildings. Likewise, there are devices and technologies whose efficiency can be affected by climatic conditions. Additionally, some electricity tariffs – such as tariffs with hourly discrimination- also have a temporary dependence. For this reason, the analysis of the energetic behavior of buildings and their installations must be carried out for a minimum period of one year.

This type of studies has, in most cases, an hourly basis. A sub-hourly basis is used when transient behavior is analyzed, such as the start-up and shutdown processes of devices or the charge and discharge of buffer tanks [29].

An hourly-based MILP optimization considering the annual behavior of the installation requires big computational costs. This calculation time increases linearly with the number of constraints and exponentially with the number of integer variables, so the resolution of a MILP model of these dimensions is not feasible in a reasonable time.

Apart from this, not all the constraints of a thermal installation have the same hourly basis. For instance, the operation condition in an hour may sometimes depend on the previous hour, as is the case of the start-up and shutdown processes of engines, thermal storage, the minimum time of operation required by some devices, etc. Moreover, there are also some constraints with an annual basis, such as legal requirements: minimum efficiencies to be guaranteed, minimum DHW to be covered by renewable or high efficiency systems, minimum percentage of primary energy savings, etc. Using constraints with different time bases means that the annual optimum will not correspond to the sum of the hourly optimums, which would considerably reduce the calculation time.

For this reason, it is necessary to reduce the size of the problem by selecting a few representative days. The number of representative days has to ensure reliable results and fit the annual values of the model, while decreasing the computational time.

Different methods have been used for selecting representative days in distributed generation systems. Some authors use three representative days that take into account the hourly and seasonal variations of the thermal demands (winter, summer, spring-autumn) [30, 31].

In [32], a graphic method based on the reproduction of the monotonic demand curve for the defined representative days is used. The analysis is applied to the optimization of a trigeneration system, considering 5, 7 and 10 representative days. Then, the number of times that each representative day is repeated throughout the year is calculated, thus obtaining a monotonic curve for each energy demand.

It is also common to use 12 representative days, one for each month of the year [33, 34]. In [33], a more compact model is proposed, where one representative day per month is initially considered and these are then classified according to climatic similarities, finally obtaining 6 representative days per year. A method for creating a seasonal representative day is also proposed. For instance, in winter, this day represents the period of heating and is created based on the maximum heating demand hour. The demand for the remaining hours is calculated as the hourly average value calculated for the heating period. In order to smooth the demand profile around the maximum load, the demand of the 2 hours before and after the peak demand is calculated as the weighted sum, giving more weight to the demand of the month where the peak demand was registered. In the case of the previous and subsequent hours, a weight of 75% is assigned to the maximum demand month and 25% to the rest of the months; whereas the hours immediately before and after these are weighted with 50% for all months. Due to the weighting, the daily energy consumption of the seasonal representative day is greater than the average energy consumption, so

the demand of the unweighted hours is proportionally reduced. This procedure can be applied to calculate the representative day of any period of time.

Other studies propose adding the days of maximum demand for heating and cooling as representative days [35], or to define 2 representative days per month, 24 days per year, in order to differentiate between working days and holidays [36].

In some studies, the influence of the number of representative days on the results of a linear optimization model is analyzed. In [37, 38], for example, the optimization is applied to a centralized thermal installation of a technology park, where there are mostly office buildings whose hourly cooling and heating demands are known. The selection of the representative days is carried out by grouping the days (objects) according to their demand and the selection of the representative day (object) of each group. This element, which is called medoid, is the center of a cluster or group. When the real demand is compared with the curve obtained with the representative days, the error diminishes whenever the number of representative days increases. As a result, a selection of 12-20 representative days is enough to obtain a reasonably good fit to the distribution of the thermal demand in central heating and cooling systems. In article [12], the number of representative days is determined for the case of a trigeneration installation in the tertiary sector. It is concluded that the results obtained for a number of representative days between 15 and 20 are more precise; whereas, for 30 representative days, the computational time increases considerably. A range of 24-30 representative days is finally proposed to obtain accurate results.

The method proposed for the selection of the representative days is based on choosing one representative day for every month, which represents the average daily demand. Likewise, the maximum thermal demand day is considered as a representative day by itself. A daily profile per month is considered for the demands of DHW and electricity, whereas the heating demand is variable for all days. Thus, 13 representative days have been selected for heating demand – including the maximum demand day – and 12 representative days are selected for DHW and electricity demands, as well as for climate data, calculated as the average day of the considered month.

For the heating demand, the representative day for each month is calculated as the average vector (centroid) for that period. Unlike the medoid, the centroid is not an object of the data set. The selection of the centroid method is justified by the Chebyshev theorem, which establishes that the centroid is the element that presents the minimum distance with respect to the other elements of the group. In the case of the month with the maximum demand day, two representative days are considered: the peak demand day and the representative day of the remaining days, calculated as the average day of the month without including the maximum demand day. With the proposed method, both the peak demand – required for the sizing of the plant – and the annual demand are kept.

In this paper, the optimization method is applied to a residential building with 36 social housings located in Bilbao (northern Spain), whose envelope has been retrofitted. The renovation works include the insulation placement, the replacement of the windows and the improvement of the air tightness. The average constructed area of a social housing is 52m^2 and the floor to ceiling height is 2.4 m. According to these data, the heating demand has been calculated using the Trnsys 17 simulation software in the document [39].

In Fig. 7, the comparative between the monotonic curve of the simulated and the representative demands is shown. As can be seen, the representative curve fits the simulated data with slight differences in low thermal powers. For this reason, the proposed method can be considered valid, due to the fact that the accuracy when increasing the number of representative days implies a greater computational time.
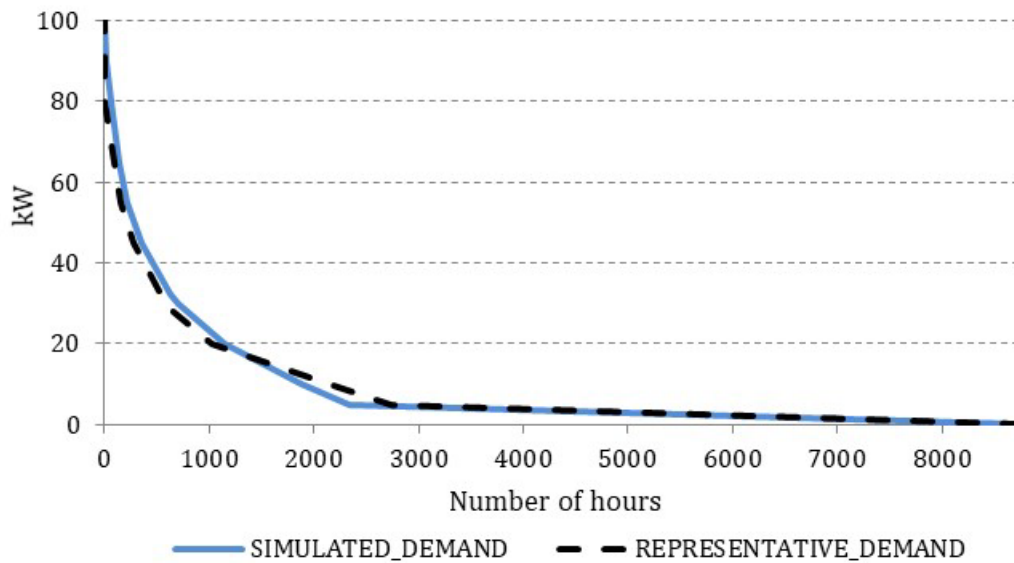
Fig. 7. Simulated and representative monotonic curves for 36 housings in Bilbao

3.2. Case study

In order to determine the influence TES systems have on the sizing and feasibility of micro-CHP plants, four different configurations have been analyzed. Once the best configuration has been determined, how the capacity of the TES affects the technical and economic feasibility of the plant is then analyzed. For this purpose, the following aspects have been considered:

- Configuration of the plant: integration of micro-CHP unit, TES system and auxiliary boiler
- Auxiliary boiler capacity
- Thermal demand covered by the TES (heating + DHW)
- Primary energy savings and CO_2 emissions avoided
- Number of operation hours and number of on-off cycles
- Installation payback and Net Present Value (NPV)

These aspects are analyzed for a particular case study, obtaining results that can be applicable and useful for installations with similar characteristics. In this case, the micro-CHP installation has been designed to meet the thermal demands of the aforementioned building located in Bilbao. All the electricity produced by this installation is considered to be self-consumed by both the end-users and the plant itself.

The monotonic curve of the heating demand is that represented in Fig. 7. The DHW hourly consumption in liters is calculated using daily and monthly multiplier factors [40], and the consumption estimated by the Spanish Technical Building Code (CTE) of 28 liters/(person·day) in the case of multifamily dwellings [41]. The DHW supply temperature is assumed to be between 60°C and 80°C to prevent legionellosis, as determined by RD 865/2003 [42]; whereas the monthly average temperature of cold water is that provided by the CTE. Regarding the electricity demand, it has been defined by means of the daily and annual profiles and by estimating the average annual electricity demand of 3500kWh for a dwelling unit of a multifamily building in Bilbao [43].

On the other hand, the micro-CHP plant includes a micro-CHP unit and a natural gas condensing boiler. Both operate at conventional high temperature ranges, that is, from 60°C to 80°C. The micro-CHP unit selected, sized according to the maximum area rectangle method, is a Senertec Dachs™ engine, which produces 12.5kW and 5.5kW of thermal and electric power, respectively, with a nominal fuel consumption of 20.5 kW. This is a one-cylinder four-stroke engine with a rated speed of 2450 rpm. Its selection responds to the fact that it is the most widespread unit in this kind of applications in Europe, leading the market of micro-CHPs in the residential and tertiary sector, with more than 20,000 installed units [29]. This unit operates at full load with no modulation possibility. The selected unit is the same for all the cases analyzed. Once the micro-CHP unit has been selected,

13

different plant configurations, depending on the integration of the TES, have been analyzed. Thus, the behavior of the TES for each of the configurations can be compared, as well as the sizing and operation of the whole plant.

The selection of a condensing boiler as an auxiliary system for this range of temperature is justified by the efficiency requirements established by the Royal Decree 238/2013 [44], condensing boilers being the only option for fulfilling the normative when the installation operates at high temperature. As shown in Appendix B, there are no significant variations in the thermal efficiency of condensing boilers in relation to the load factor at high temperature, so the condensing boiler is assumedto have constant thermal efficiency. The nominal thermal power of the boiler is not previously determined, but after the linear optimization, which also determines the arrangement of the thermal storage and its volume. In order to observe their influence, the nominal power of the micro-CHP engine is not modified.

The size and operation of the proposed configurations have been optimized according to an economic criterion, considering that the thermal demand is completely satisfied and that the generated electricity is self-consumed within the building. MILP algorithms have been used, it being necessary to linearize all the non-linear problems. The 24-hour horizon (with 24 steps of one-hour) is considered to guarantee an efficient use of energy resources and a greater value of the PES, due to the reduction of heat losses in the TES and the augmentation of useful heat.

Integration of TES

In this work, four different configurations have been analyzed, depending on how the TES is integrated and its operation mode. These configurations are detailed in Section 2.3:

- **Configuration 0.** Micro-CHP plant without thermal storage (Fig. 8): the useful thermal energy is the heat produced by the micro-CHP unit. The peak loads are supplied by the condensing boiler.
- **Configuration 1.** Micro-CHP plant with TES arranged in series in the return circuit (Fig. 9): the thermal energy generated in the micro-CHP unit can be charged or used directly to meet the thermal demand. When the stored energy is discharged, the useful heat of the micro-CHP is the sum of the discharged energy and the heat produced by the micro-CHP unit. Thus, the TES cannot be simultaneously charged and discharged.
- **Configurations 2 and 3.** Micro-CHP plant with TES arranged in parallel (Fig. 10): as the micro-CHP unit is directly connected to the TES, the heat produced by the micro-CHP unit is always charged. Therefore, the useful heat provided by the micro-CHP unit corresponds to the discharged energy. In Configuration 2, it is considered that the production and the thermal demand are uncoupled for a period of time, so charging and discharging cannot happen at the same time. In case of Configuration 3, there is no restriction on simultaneous charging and discharging.
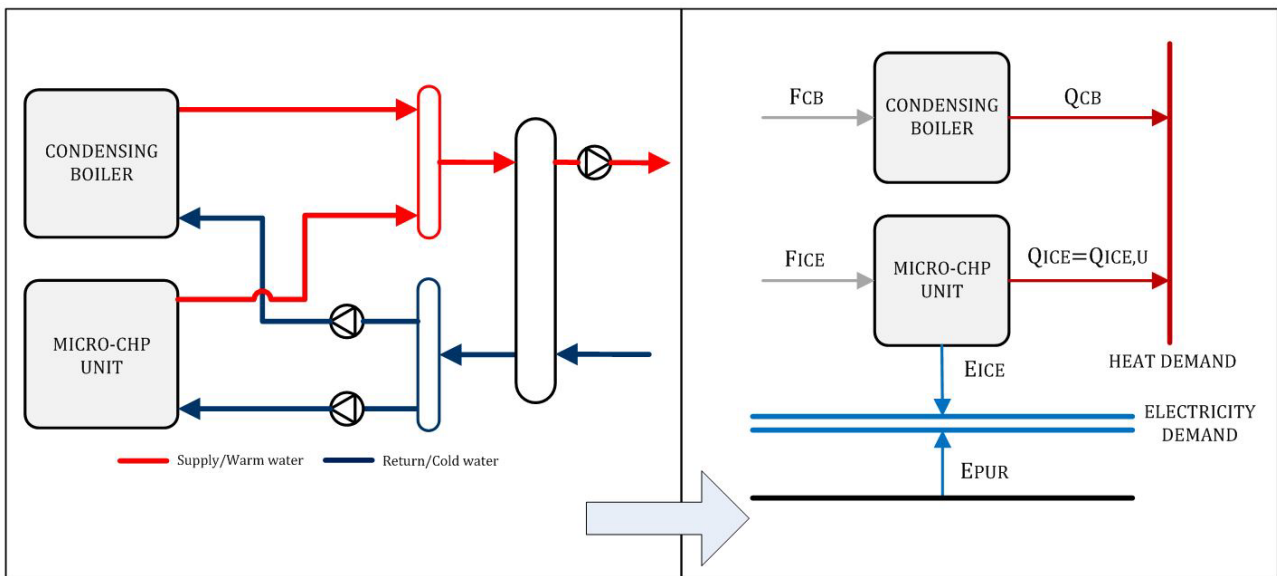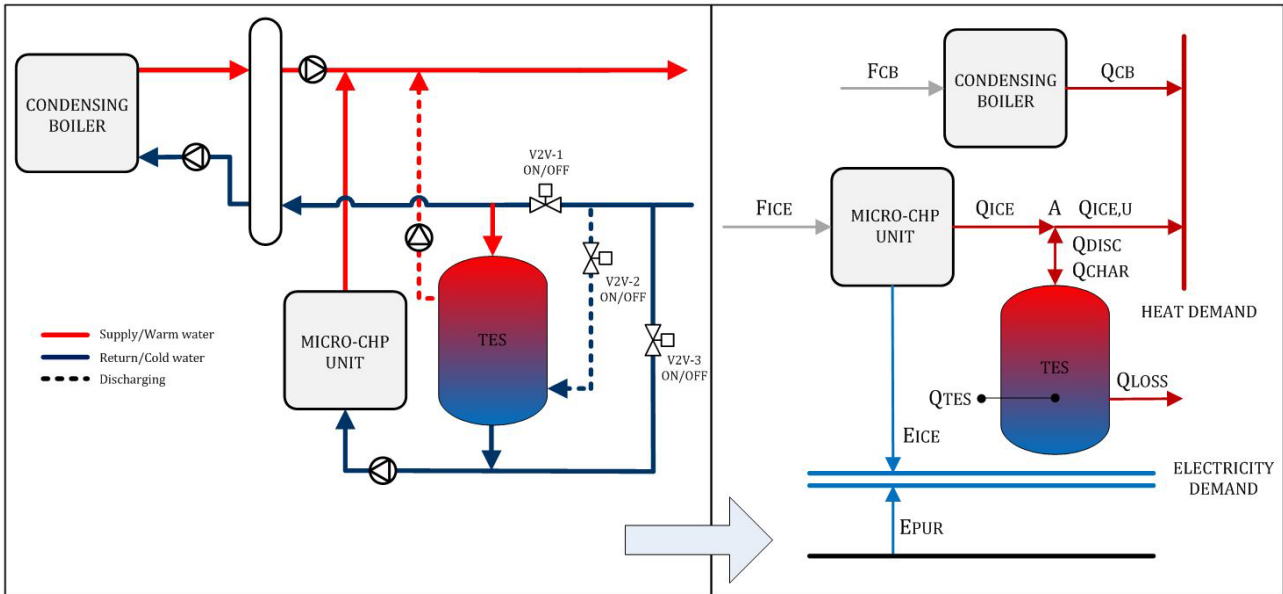
-

Fig. 8. Configuration 0: without TES

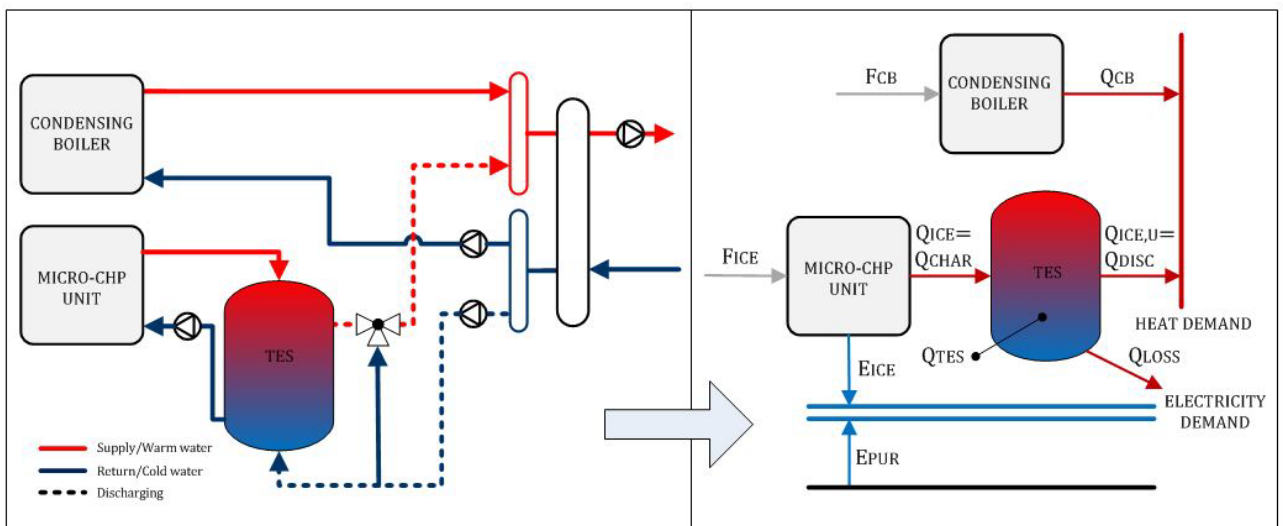**Fig. 9. Configuration 1: with TES arranged in series in the return circuit**

Fig. 10. Configurations 2 and 3: with TES arranged in parallel

3.3. Economic and environmental analysis

To tackle the economic analysis, electricity and natural gas tariffs, as well as the investment and maintenance costs of the device, must be defined. The purchase price of electricity established by the last resource tariff (TUR) comes to 12.411 c€/kWh, while that corresponding to natural gas for the final user is 5.726 c€/kWh. Likewise, the maintenance cost of the micro-CHP unit is considered to be variable with the electricity generation (2.5 c€/kWh$_e$) [45].

Regarding investment costs, only the initial cost of the device that has to be sized –boiler and TES– is taken into account, since the cost of the micro-CHP unit is constant in all configurations. For that purpose, the "cost-thermal power" ($C_{CB}=f(\dot{Q}_{CB\_NOM})$) and the "cost-volume" ($C_{TES}=f(V_{TES})$) linear functions are defined for the condensing boiler and the buffer tank, respectively (Appendix B).

The environmental analysis focuses on the calculation of greenhouse gas (GHG) emissions. According to the Spanish Institute for Energy Saving and Diversification [46], equivalent CO_2 emissions of the energy resources consumed within the plant are 399 g of CO_{2eq}/kWh for grid electricity and 252 g of CO_{2eq}/kWh for the combustion of natural gas. Equivalent CO_2 emissions and energy consumption during the manufacturing of the device are not

considered. This assumption is supported by the fact that the manufacturing of non-renewable thermal systems represents less than 2% of the total environmental impact during their life cycle [47].

3.4. Linear optimization model

The optimization problem consists of minimizing the objective function, C_{TOT}, that represents the global annual cost of the micro-CHP installation. This global cost includes the annual amortization of the initial investment, C_{INV}, and the variable cost due to the operation and maintenance of the plant, $C_{O\&M}$. Thus, the objective function is defined as follows:

$$Min\ C_{TOT} = C_{INV} + C_{O\&M}$$

Eq. 5

The annual amortization of investment, C_{INV}, is calculated as the product of the capital recovery factor (*CRF*) of each technology k and the investment cost of the previously mentioned technologies. Whilst this cost only considers the investment of the boiler and the TES system, the cost of the engine and its corresponding retribution to investment are not taken into consideration, since they are common to all the analyzed cases. Furthermore, maintenance costs of the boiler and the TES are not explicitly considered, but as a function of the investment cost (Appendix B).

$$C_{INV} = \sum_k \left(CRF_k \cdot C_k + C_{FM,k} \right)$$

Eq. 6

On the other hand, the CRF factor is calculated as follows:

$$CRF_k = \frac{i \cdot (1 + i)^{n_k}}{(1 + i)^{n_k} - 1}$$

Eq. 7

where i is the effective annual interest rate and n_k is the lifetime of each technology k. The assumed value for the interest rate is 5 % [48, 49], whilst a lifetime of 15 years is considered for the thermal installation.

Operational and maintenance costs are lumped together within a variable cost which is calculated as the hourly sum of the product between the hourly operational and maintenance costs for the representative day and the column vector *ntd(d)*, which represents the number of times that each representative day is repeated during a year.

$$C_{O\&M} = \sum_d \sum_h C_{O\&M}(d, h) \cdot ntd(d)$$

Eq. 8

$C_{O\&M}(d,h)$ includes both the cost of the energy resources –natural gas consumption of the ICE and the boiler, c_F, and the electricity supplied by the grid, c_E–, as well as the variable maintenance cost of the device, $C_{VM}(d,h)$, which depends on its operation. In this case, $C_{VM}(d,h)$ mainly refers to the maintenance of the micro-CHP unit, the value provided by the manufacturer being a function dependent on the amount of electricity generated. Since all the electricity generated is considered to be self-consumed, the retribution to the ICE operation is not taken into account.

$$C_{O\&M}(d, h) = c_F \cdot \left(F_{CB}(d, h) + F_{ICE}(d, h) \right) + c_E(d, h) \cdot \left(E_{DEM}(d, h) - E_{ICE}(d, h) \right) + C_{VM}(d, h)$$

Eq. 9

$$C_{VM}(d, h) = C_{VM\_ICE}(d, h) = f \left(E_{VM\_ICE}(d, h) \right)$$

Eq. 10

Other linear equations and inequalities are obtained from the energy balance of each technology, its capacity and production limits, and the fulfillment of the regulation in force.

3.4.1. Technical and economic constraints

3.4.1.1. Internal Combustion Engine

The operation cost of the ICE is the annual cost associated to its fuel consumption. As the selected engine only operates at full load, the overall fuel consumed by the engine is calculated as the product between the nominal

consumption, $\dot{F}_{ICE\_NOM,}$ for one hour and a binary variable, *ICE(d,h)*. This variable indicates whether the engine is operating in the *h* hour of the *d* day.

$$F_{ICE}(d,h) = ICE(d,h) \cdot \dot{F}_{ICE\_NOM} \cdot t \qquad \text{Eq. 11}$$

$$ICE(d,h)\ bin \qquad \text{Eq. 12}$$

As a general rule, thermal and electrical production are calculated from thermal and electrical efficiencies (η_Q and η_E), respectively:

$$E_{ICE}(d,h) = F_{ICE}(d,h) \cdot \eta_E \qquad \text{Eq. 13}$$

$$Q_{ICE}(d,h) = F_{ICE}(d,h) \cdot \eta_Q \qquad \text{Eq. 14}$$

Nevertheless, the transient behavior during start-up and shutdown periods of the engines implies a decrease in electrical and thermal efficiency. In the ANNEX 42 workgroup of the IEA – ECBCS program (International Energy Agency's Energy and Buildings Communities Program), the modeling and calibration of a Senertec Dachs engine was carried out, with the corresponding validation of the model [50]. This research took into consideration the dynamic response of the engine in cold and hot start conditions, as well as during the shutdown process.

In the proposed optimization model, the drop in efficiency that takes place during the start-up phase, which was characterized within the Annex 42 framework, is modeled as a penalty applied to both heat and electricity production. The effects of the engine shutdown, on the other hand, have not been considered, since their influence is lower than 1% [50]. As mentioned above, the continuous operation of the engine guarantees a greater useful life of the device and the viability of the micro-CHP, which is intimately related to the number of hours of operation of the unit. For these reasons, it is consideredthat the unit never spends enough time in standby mode after turning off to reach ambient conditions and it always starts in warm conditions. Therefore, the decrease in the thermal production is approximately 8%; whereas the electricity production is reduced by 5%, according to values extracted from [50] for the aforementioned conditions.

The efficiency-related penalty has only been applied in the start-up, that is, when *ICE(d,h-1)* is 0 and *ICE(d,h)* is 1. In any other case, no penalty is applied, since the engine will continue to operate in a continuous way *(ICE(d,h-1)=1; ICE(d,h)=1)*, or it will turn off (*ICE(d,h-1)=1; ICE(d,h)=0*). Additionally, it is considered that the engine is initially off at the beginning of every representative day (*ICE(d,0)*). The difference between the engine state in the *h* hour and the state in the *h-1* hour for the *d* day is represented by the function *x(d,h)*.

$$x(d,h) = ICE(d,h) - ICE(d,h-1) \qquad \text{Eq. 15}$$

$$ICE(d,0) = 0 \qquad \text{Eq. 16}$$

Likewise, a function that represents the start-up process of the engine is also defined. This function, shown in Fig. 11, takes the value 1 when the engine starts (*x(d,h)=1*) and 0 in the remaining cases:

$$start\_up(x) = \begin{cases} 0; & when\ x = x_1 = -1\ (shutdown) \\ 0; & when\ x = x_2 = 0\ (operation\ mode\ does\ not\ vary) \\ 1; & when\ x = x_3 = 1\ (starting) \end{cases} \qquad \text{Eq. 17}$$
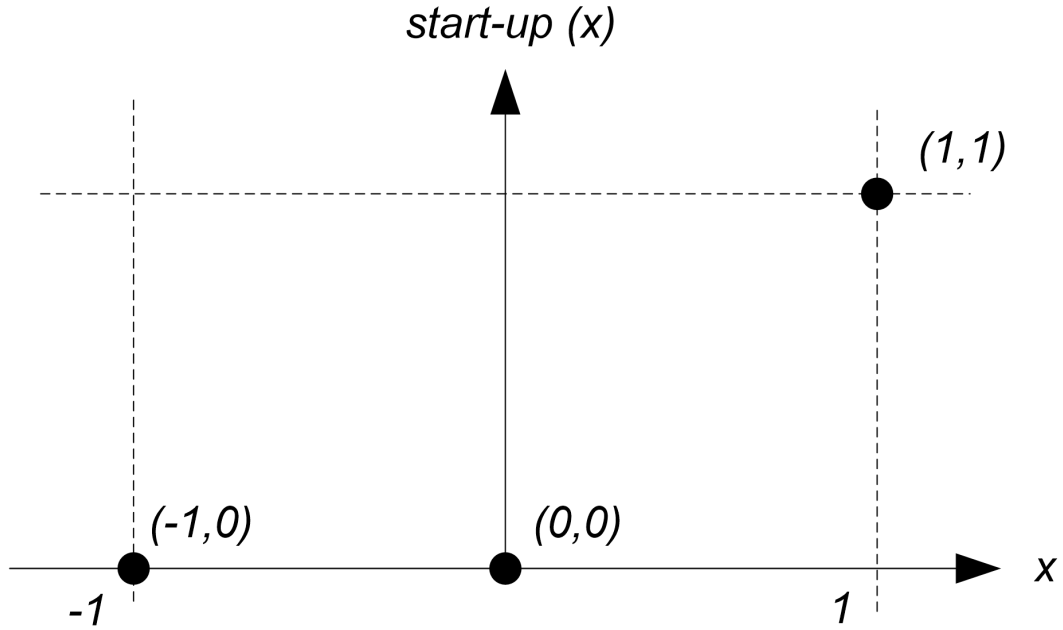
Fig. 11. Start-up discontinuous function

Start-up(x) is a discontinuous nonlinear function represented by an if-then-else expression. In order to linearize and reformulate this if-then-else statement, binary variables are used.

As shown in Eq. 17, the penalty is considered when $x(d,h)=x_3(d,h)$. The binary variables $(\delta_1(d,h), \delta_2(d,h), \delta_3(d,h))$ are defined to determine when the start-up takes place and to apply the corresponding penalty, as only one of these binary variables is positive in the considered instant.

$$\delta_1(d,h), \delta_2(d,h), \delta_3(d,h) \quad bin \qquad \text{Eq. 18}$$

$$\delta_1(d,h) + \delta_2(d,h) + \delta_3(d,h) = 1 \qquad \text{Eq. 19}$$

$$x_1(d,h) = -\delta_1(d,h) \qquad \text{Eq. 20}$$

$$x_2(d,h) = 0 \qquad \text{Eq. 21}$$

$$x_3(d,h) = \delta_3(d,h) \qquad \text{Eq. 22}$$

$$x(d,h) = x_1(d,h) + x_2(d,h) + x_3(d,h) \qquad \text{Eq. 23}$$

$$start\_up(d,h) = \delta_3(d,h) \qquad \text{Eq. 24}$$

According to the characterization results [50], the electricity penalty in the Dachs engine during the start-up period, PSU_E, and the thermal energy penalty, PSU_Q, are the following:

$$PSU_E = 0.05 \qquad \text{Eq. 25}$$

$$PSU_Q = 0.08 \qquad \text{Eq. 26}$$

$$E_{ICE}(d,h) = (ICE(d,h) - start\_up(d,h) \cdot PSU_E) \cdot F_{ICE\_NOM} \cdot \eta_E \qquad \text{Eq. 27}$$

$$Q_{ICE}(d,h) = \left(ICE(d,h) - start\_up(d,h) \cdot PSU_Q\right) \cdot F_{ICE\_NOM} \cdot \eta_Q \qquad \text{Eq. 28}$$

3.4.1.2. Thermal Storage System (TES)

In this section, the previously proposed configurations for integrating TES in micro-cogeneration plants are described and modeled.

Configuration 0: no TES

In the case of Configuration 0, no thermal storage system is installed, so all the useful heat is provided by the engine in the considered instant.

$$Q_{ICE}(d,h) = Q_{ICE,U}(d,h) \qquad \text{Eq. 29}$$

Configuration 1: TES arranged in series in the return circuit

In this case, TES is integrated in the return circuit according to Fig. 9. Applying the energy balance in node A:

$$Q_{ICE}(d,h) + Q_{DISCH}(d,h) = Q_{CHAR}(d,h) + Q_{ICE,U}(d,h) \qquad \text{Eq. 30}$$

Heat stored every hour, $Q_{STO}(d,h)$, is obtained from the energy balance in the tank (Eq. 31), where thermal losses, $Q_{LOSS}(d,h)$, are estimated to be 1% of the total thermal energy content of the tank in the previous instant, as defined in Eq. 32. The average percentage of losses is calculated in Appendix B for different types of insulation, diameter-to-height ratio and average temperature of the storage medium.

$$Q_{STO}(d,h) = Q_{STO}(d,h-1) + Q_{CHAR}(d,h) - Q_{DISCH}(d,h) - Q_{LOSS}(d,h) \qquad \text{Eq. 31}$$

$$Q_{LOSS}(h) = 0.01 \cdot Q_{STO}(d,h-1) \qquad \text{Eq. 32}$$

As charging and discharging processes cannot happen simultaneously, it is necessary to use the binary variables *CHAR(d,h)* and *DISCH(d,h)* to represent if either the charging or discharging processes, respectively, are active. When one of these is 1, the other one has to be 0 and vice versa, so the sum of these variables will not be greater than 1.

$$CHAR(d,h), DISCH(d,h) \ bin \qquad \text{Eq. 33}$$

$$CHAR(d,h) + DISCH(d,h) \leq 1 \qquad \text{Eq. 34}$$

Likewise, when the TES system is charging (CHAR(d,h)=1), the heat provided to the tank must be equal to or lower than the heat generated by the ICE in the considered instant.

$$Q_{CHAR}(d,h) \leq CHAR(d,h) \cdot Q_{ICE}(d,h) \qquad \text{Eq. 35}$$

Due to the fact that both *CHAR(d,h)* and $Q_{ICE}(d,h)$ are variable over the time, their product is non-linear. In order to linearize this product, the big M method was used, as explained in Appendix A. This method consists of taking a high value constant (*M*), which lets the constraint move outside the limits of the region inscribed by the problem constraints.

$$Q_{CHAR}(d,h) \leq M \cdot CHAR(d,h) \qquad \text{Eq. 36}$$

As mentioned above, the charged heat has to be lower than the heat generated by the engine:

$$Q_{CHAR}(d,h) \leq Q_{ICE}(d,h) \qquad \text{Eq. 37}$$

If these equations are applied to the case in which heat is not charged (*CHAR(d,h)*=0), and considering that all the variables are non-negative, the only value that $Q_{CHAR}(d,h)$ can take is 0. Otherwise, (*CHAR(d,h)*=1), the value of $Q_{CHAR}(d,h)$, will be between 0 and $Q_{ICE}(d,h)$.

When the tank is being discharged (*DISCH(d,h)*=1), the heat content of the tank in the analyzed instant cannot be greater than that in the previous instant.

$$Q_{DISCH}(d,h) \leq DISCH(d,h) \cdot Q_{STO}(d,h-1)$$ Eq. 38

Thus, a product of variables is obtained that has to be linearized using the big-M method:

$$Q_{DISCH}(d,h) \leq M \cdot DISCH(d,h)$$ Eq. 39

$$Q_{DISCH}(d,h) \leq Q_{STO}(d,h-1)$$ Eq. 40

Furthermore, it is considered that there is no heat stored in the tank in the initial instant. The heat stored at every instant must be lower than the capacity of the TES system, Q_{CAP}, which is another variable dependent on the TES volume, V_{TES}.

$$Q_{STO}(d,0) = 0$$ Eq. 41

$$Q_{STO}(d,h) \leq Q_{CAP}$$ Eq. 42

The storage capacity is calculated considering a temperature difference between the top and bottom of the stratified thermal storage tank of 13°C, which is the temperature difference of the cooling water between the outlet and the inlet in the Senertec Dachs engine when working with constant flow [50].

Configuration 2: TES arranged in parallel. No possibility of simultaneous charging and discharging.

As can be observed in Fig. 10, in the case of Configurations 2 and 3, where the engine is directly connected to the buffer tank, all the thermal energy generated in the ICE is charged into the tank. In Configuration 2, since charging and discharging cannot occur simultaneously, all the heat produced is stored, and discharged whenever the ICE is off and there is need for thermal energy. The discharged thermal energy corresponds to the useful heat supplied by the engine, $Q_{ICE,U}(d,h)$.

$$Q_{CHAR}(d,h) = Q_{ICE}(d,h)$$ Eq. 43

$$Q_{DISCH}(d,h) = Q_{ICE,U}(d,h)$$ Eq. 44

As charging and discharging cannot take place simultaneously, it is necessary to use both the *CHAR(d,h)* and *DISCH(d,h)* binary variables used in Configuration 1 to determine which process is taking place. For that, the mathematical model includes Equations 33, 34, 35, 36, 38, 41 and 42. The thermal balance and losses of the TES system are calculated with Eq.31 and Eq.32 defined in Configuration 1.

Configuration 3: TES arranged in parallel. Possibility of simultaneous charging and discharging.

This configuration differs from Configuration 2 in the possibility of simultaneous charging and discharging of the tank. For this reason, the *CHAR(d,h)* and *DISCH(d,h)* binary variables are not necessary, so the mathematical model is defined by means of equations 31, 32, 41, 42, 43 and 44.

The cost of the tank is calculated from the function ($C_{TES}=f(V_{TES})$) shown in Appendix B. This linear function has been obtained through a linearization by segments (Appendix A).

$$C_{TES} = 3.1635 \cdot x_1 + 1.7601 \cdot x_2 + 701.69 \cdot \lambda_2 + 1.0360 \cdot x_3 + 1358.3 \cdot \lambda_3$$ Eq. 45

$$V_{TES} = x_1 + x_2 + x_3$$ Eq. 46

$$\lambda_1, \lambda_2, \lambda_3 \; bin$$ Eq. 47

$$\lambda_1 + \lambda_2 + \lambda_3 = 1$$ Eq. 48

$$0 \leq x_1 \leq 500 \cdot \lambda_1$$ Eq. 49

$$500 \cdot \lambda_2 \leq x_2 \leq 1000 \cdot \lambda_2 \qquad \text{Eq. 50}$$

$$1000 \cdot \lambda_3 \leq x_3 \leq 5000 \cdot \lambda_3 \qquad \text{Eq. 51}$$

3.4.1.3. Condensing Boiler (CB)

The thermal energy produced during one hour in the condensing boiler, $Q_{CB}(d,h)$, has to be equal to or lower than the thermal energy produced for one hour if it operates at nominal thermal power, $\dot{Q}_{CB\_NOM}$, which is also a variable. The fuel consumption, $F_{CB}(d,h)$, is calculated considering an average thermal efficiency of the condensing boiler of 97.8% (Appendix B), calculated for supply and return temperatures of 80°C and 60°C, respectively.

$$Q_{CB}(d,h) \leq \dot{Q}_{CB\_NOM} \cdot t \qquad \text{Eq. 52}$$

$$F_{CB}(d,h) = \frac{Q_{CB}(d,h)}{\eta_{CB}} \qquad \text{Eq. 53}$$

The cost of the condensing boiler is a function of the nominal thermal power (Appendix B):

$$C_{CB} = \left(39.416 \cdot Q_{CB\_NOM} + 8771.6\right) \qquad \text{Eq. 54}$$

3.4.1.4. Thermal energy supply

The thermal demand is the sum of heating ($Q_{HEAT}(d,h)$) and hot water ($Q_{DHW}(d,h)$) demands. It is supplied by means of the useful heat provided by the engine, $Q_{ICE,U}(d,h)$, and the condensing boiler, $Q_{CB}(d,h)$.

$$Q_{DEM}(d,h) = Q_{HEAT}(d,h) + Q_{DHW}(d,h) \qquad \text{Eq. 55}$$

$$Q_{DEM}(d,h) = Q_{ICE,U}(d,h) + Q_{CB}(d,h) \qquad \text{Eq. 56}$$

3.4.1.5. Electricity supply

As the electricity generated in the engine, $E_{ICE}(d,h)$, is assumed to be self-consumed, it will be lower than the total electricity demand, meeting the difference between demand and production with electricity purchased from the grid ($E_{PUR}(d,h)$).

$$E_{DEM}(d,h) = E_{ICE}(d,h) + E_{PUR}(d,h) \qquad \text{Eq. 57}$$

$$E_{PUR}(d,h) \geq 0 \qquad \text{Eq. 58}$$

3.4.2. Legal constraints

The Spanish Technical Building Code [41] imposes a minimum coverage of the DHW demand by means of high efficiency or renewable technologies. In the case of Bilbao, this minimum contribution is 30%, so the annual useful heat of cogeneration must be greater than this value.

$$\sum_h Q_{ICE,U}(d,h) \geq 0.30 \cdot \sum_d \sum_h Q_{DHW}(d,h) \qquad \text{Eq. 59}$$

According to Directive 2012/27/EU [51], in order to consider micro-CHP as high efficiency cogeneration, the micro-CHP unit should achieve primary energy savings compared to the separate production of heat and electricity through conventional ways. Thus, the primary energy saving (PES) has to be positive.

$$PES \, (\%) = \left(1 - \frac{1}{\frac{\eta_Q}{Ref\, H_\eta} + \frac{\eta_E}{Ref\, E_\eta}}\right) \cdot 100 \geq 0 \qquad \text{Eq. 60}$$

where η_Q and η_E are the annual thermal and electric efficiencies of the micro-cogeneration production, and $Ref\,H_\eta$ and $Ref\,E_\eta$ are the harmonized reference efficiencies for the separate production of heat and electricity established by the European Commission [52]. These harmonized reference values are assumed to be 45% for the separate production of electricity –including grid losses– and 90% for the separate production of heat through a natural gas boiler.

As mentioned above, in cogeneration plants, when a buffer tank is installed, the useful heat is considered instead of the heat produced by the engine. Moreover, thermal and electrical efficiencies are not constant. According to these considerations, the constraint is expressed as:

$$\frac{\sum_d \sum_h Q_{ICE,U}(d,h)\,/\,\sum_d \sum_h F_{ICE}(d,h)}{RefH_\eta} + \frac{\sum_d \sum_h E_{ICE}(d,h)\,/\,\sum_d \sum_h F_{ICE}(d,h)}{RefE_\eta} - 1 \geq 0 \qquad \text{Eq. 61}$$

The PES can also be expressed in terms of energy. This concept allows the non-renewable primary energy saving of the installation under study to be calculated, considering the reference values for separate production established by the corresponding directive. The PES in MWh for the micro-CHP plant is calculated as follows:

$$PES\,(MWh) = \frac{Q_{ICE,U}}{Ref\,H_\eta} + \frac{E_{ICE}}{Ref\,E_\eta} - F_{ICE} \qquad \text{Eq. 62}$$

Furthermore, the Spanish Royal Decree 661/2007 [53] defines the cogeneration efficiency by means of the equivalent electric efficiency (REE), which compares the electricity obtained in a cogeneration installation and the electricity of a power plant where only electricity is produced. According to this Royal Decree, the REE must be greater than or equal to 49.5% in the case of natural gas micro-CHP engines.

$$REE = \frac{E_{ICE}}{F_{ICE} - \left(\frac{Q_{ICE,U}}{RefH_\eta}\right)} \geq 49.5\% \qquad \text{Eq. 63}$$

Adapting this constraint to the mathematical model, the following expression is obtained:

$$\sum_d \sum_h E_{ICE}(d,h) \geq 0.495 \cdot \left(\sum_d \sum_h F_{ICE}(d,h) - \sum_d \sum_h Q_{ICE,U}(d,h)/Ref\,H_\eta\right) \qquad \text{Eq. 64}$$

3.4.3. Economic feasibility

In order to determine the economic feasibility, the Net Present Value (NPV) is calculated. The NPV represents the current value of all the incomes and expenses during the lifetime of the installation in relation to the initial investment in the project; whereas the payback focuses on the period for recovering the investment cost. As the investment is assumed to be made at the beginning of the project, the NPV is calculated as follows:

$$NPV = -Inv + \sum_{t=1}^{t=n_k} \left[{NS}\big/{(1+r)^t}\right] \qquad \text{Eq. 65}$$

where Inv is the investment of the project in comparison with the reference plant (Configuration 0: configuration without TES), n_k is the useful life of the plant, r is the discount rate (5%) [48, 49], and NS is the net saving generated in each period t, which is calculated as the difference of the operation costs between the micro-CHP plant and the reference plant.

4. Results and discussion

In this section, the annual results of the optimization are analyzed for the considered configurations. In Table 1, the results relating to the sizing of the condensing boiler and the TES system are shown.

Table 1. Comparative between considered configurations

	Configuration 0	Configuration 1	Configuration 2	Configuration 3
E_{ICE} (MWh)	18.6	28.1	23.9	28.3
$Q_{ICE,U}$ (MWh)	42.7	64.3	52.7	64.6
F_{ICE} (MWh)	71.4	107.1	92.1	107.7
$\dot{Q}_{CB,NOM}$ (kW)	95.5	85.3	70.5	85.7
F_{CB} (MWh)	82.0	60.0	71.7	59.7
Q_{CAP} (kWh)	0.0	10.3	73.2	9.9
V_{TES} (litres)	0	683	4839	653
Operation hours of ICE	3482	5222	4492	5252
Number of start-ups of ICE	821	856	1155	763
Contribution to DHW (%)	54.7	82.6	58.6	82.8
Efficiency of the plant (%)	94.5	92.0	91.4	91.9
$C_{O\&M}$ (€)	22579	22415	22652	22411
C_{TOT} (€)	25713	25689	26137	25680
Payback (years)	-	8.9	-	8.4
NPV (€)	0.0	242	-3656	340
PES (%)	19.5	20.0	17.5	20.1
PES (MWh)	17.3	26.8	19.6	27.0
REE (%)	77.6	78.9	71.3	78.9
CO_2 avoided (ton CO_{2eq})	10.4	15.9	12.7	16.1

As can be observed, Configurations 1 and 3 are those which present better thermodynamic, economic and environmental results. The storage volume in these configurations is much lower than the optimal volume obtained for Configuration 2, where charging and discharging take place separately. This fact makes the number of start-up and shutdown periods increase considerably, despite the decrease in the operation hours. This discontinuous operation of the engine may involve a shorter lifetime, which is an important qualitative aspect to take into account.

Regarding the sizing of the boiler, its nominal power diminishes as the storage volume increases. This is why the boiler capacity in Configuration 2 is lower. Nevertheless, the higher heat losses of the TES and the lower electricity generation are not compensated for with the lower cost of the condensing boiler.

In relation to the economic aspect, Configurations 1 and 3 have a positive NPV that guarantees the feasibility of these configurations with respect to the configuration without TES. In the case of Configuration 2, the NPV is negative, which implies a lack of economic feasibility.

Besides that fact, such energy indicators as the PES and REE, as well as the avoided emissions of CO_{2eq}, are greater in Configurations 1 and 3, obtaining the lowest values with Configuration 2.

On the other hand, for a better understanding of these results, the thermal energy balances are also represented in Figures 12 to 19. In every case, the annual optimal operation mode is determined according to an economic criterion. Even though 13 representative days are selected for the optimization, for the sake of clarity, only the representative days for the maximum and minimum thermal demands (annual peak demand day on January 11th and average day of July) are shown, since these provide a general view of the optimal operation. The energy balance is depicted hourly from hour 1 to hour 24, where the value of a variable represented for hour 1 is considered to be constant from 12.00 a.m. to 1.00 a.m., and so on.

Configuration 0

As shown in Fig. 12 and Fig. 13, if no TES is installed, the ICE only runs when the thermal demand is greater than its nominal thermal power. Thereby, on the maximum demand day, the ICE operates continuously from 5.00 a.m. to 11.00 p.m. (Fig. 12); whereas, in summer, it would have a discontinuous operation, with multiple start-ups and shutdowns and few operation hours (Fig. 13).
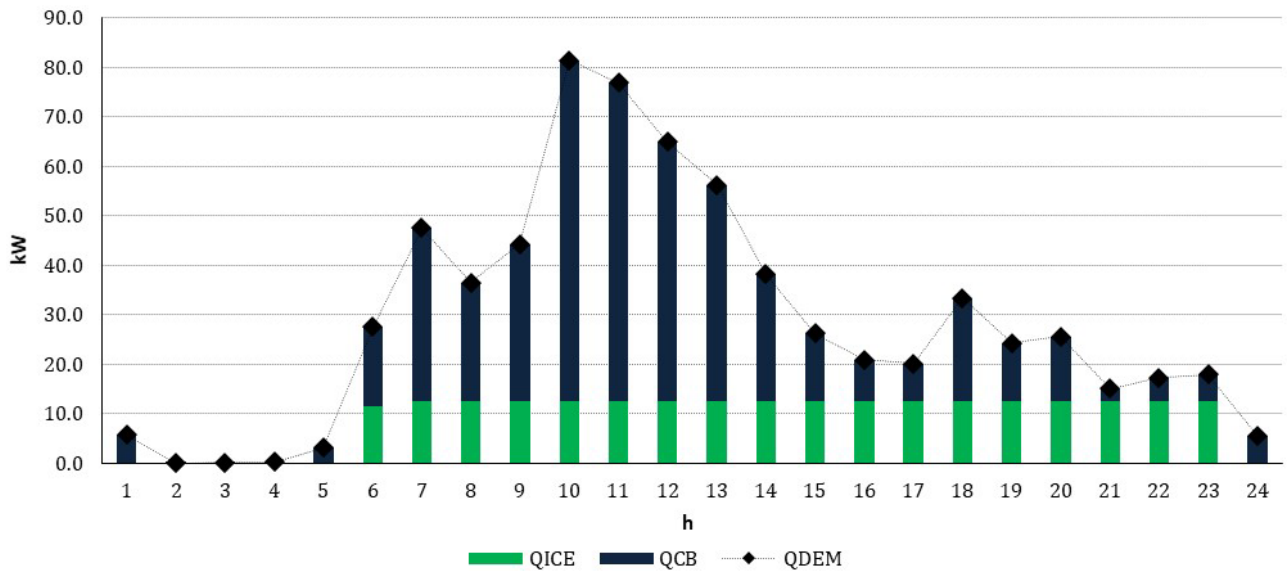
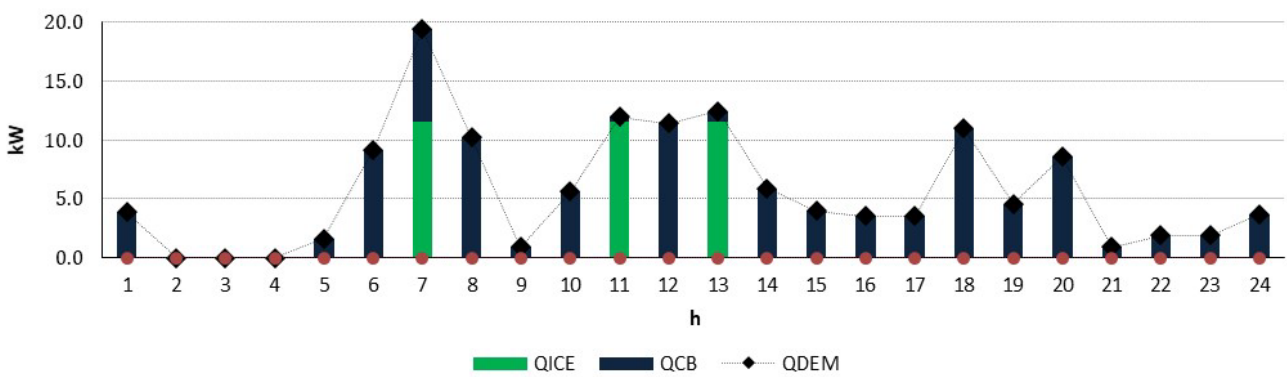**Fig. 12. Thermal balance of the maximum demand representative-day for Configuration 0**

Fig. 13. Thermal balance of the minimum demand representative-day for Configuration 0

Configuration 1

When integrating the storage in series in the return circuit, the engine operates in a continuous way from 4.00 a.m. to 11.00 p.m. on the day of maximum demand (Fig. 14). Due to the fact that the demand of this representative day is high, heat is only stored between 4.00 a.m. and 5.00 a.m. Then, in the following hour, when thermal demand increases, heat stored within the tank is discharged. If the heat content of the TES system was not discharged to be used when there is thermal demand, the heat losses of the tank would increase and the heat discharge in subsequent hours would diminish.
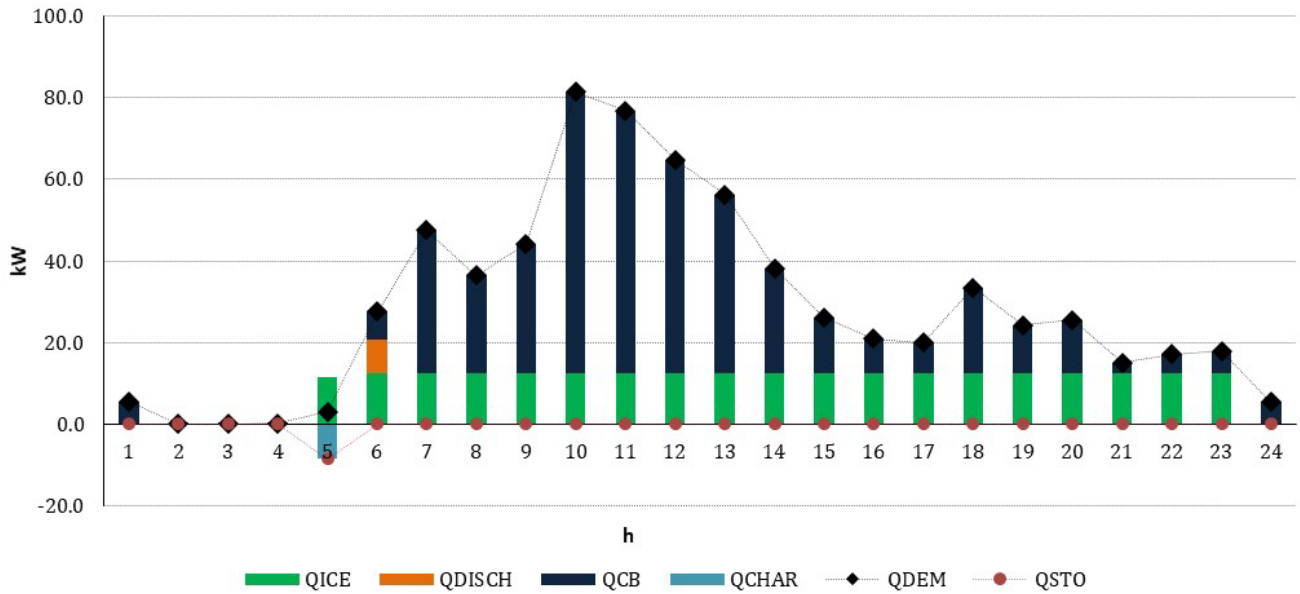
Fig. 14. Thermal balance of the maximum demand representative-day for Configuration 1

On the other hand, on the minimum thermal demand day (Fig. 15) – unlike in the configuration without storage – the engine supplies most of the thermal demand. The heat surplus is stored and discharged in those hours when the demand is lower. Thus, a more constant operation of the engine is achieved, as well as a greater number of operation hours.
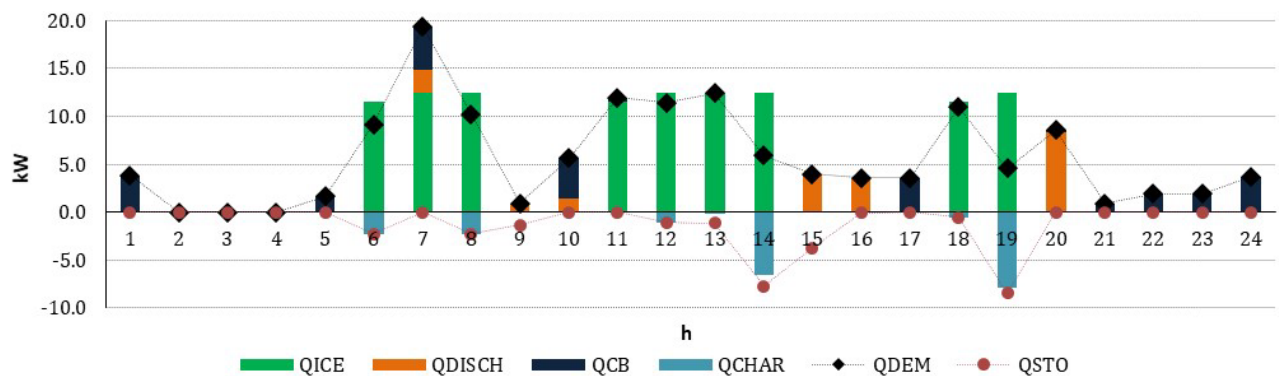

Fig. 15. Thermal balance of the minimum demand representative-day for Configuration 1

Configuration 2

In Fig. 16 and Fig. 17, where results for Configuration 2 – intermediate storage with no possibility of simultaneous charging and discharging – are depicted, it can be seen that the engine operates during the first hours of the day, accumulating the whole thermal energy production in the TES system in order to use it later on when the demand increases. Since the engine is directly connected to the tank, once the tank starts discharging, the engine is stopped. This requirement implies a greater number of start-ups and shutdowns of the engine and greater storage volumes.
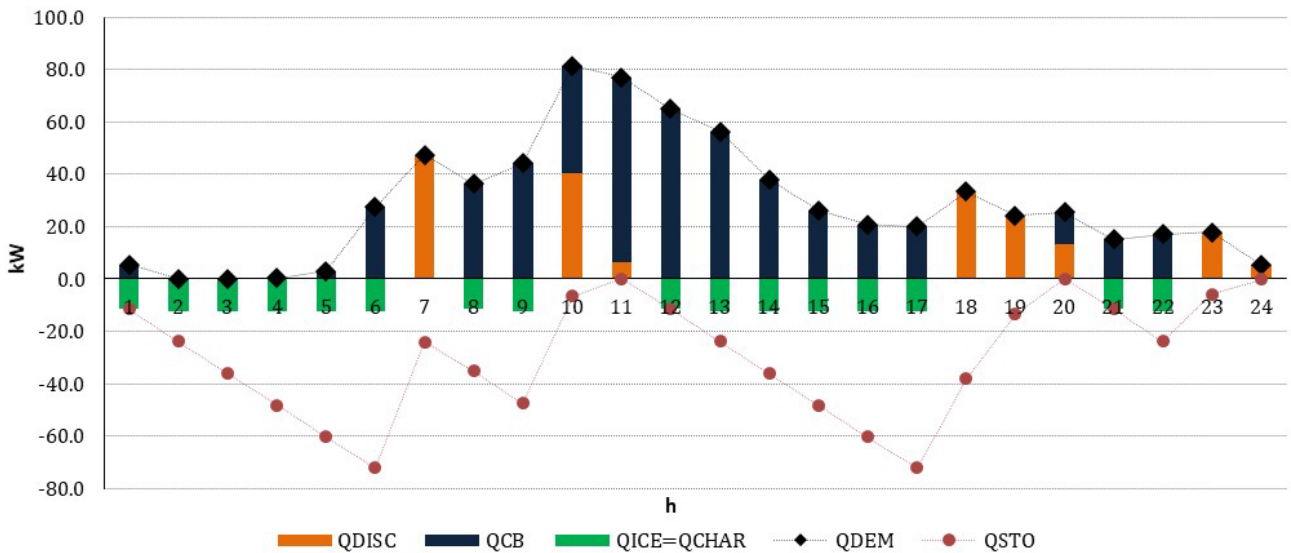
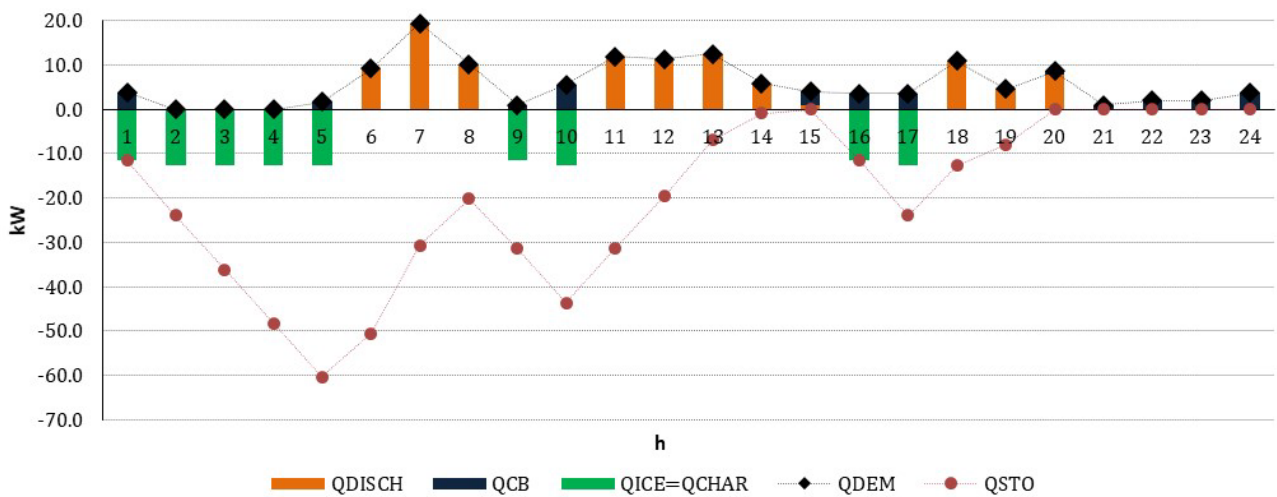Fig. 16. Thermal balance of the maximum demand representative-day for Configuration 2

Fig. 17. Thermal balance of the minimum demand representative-day for Configuration 2

Configuration 3

In Configuration 3, the intermediate integration of the TES with the possibility of simultaneous charging and discharging is analyzed. As shown in Fig. 18, the engine operates from 4.00 a.m. to 11.00 p.m. during the day of maximum thermal demand, thus ensuring a continuous functioning. In the case of the minimum demand day (Fig. 19), the engine operates to meet the thermal demand curve, charging and discharging at the same time. This fact implies lower accumulation volumes and a decrease in heat losses.
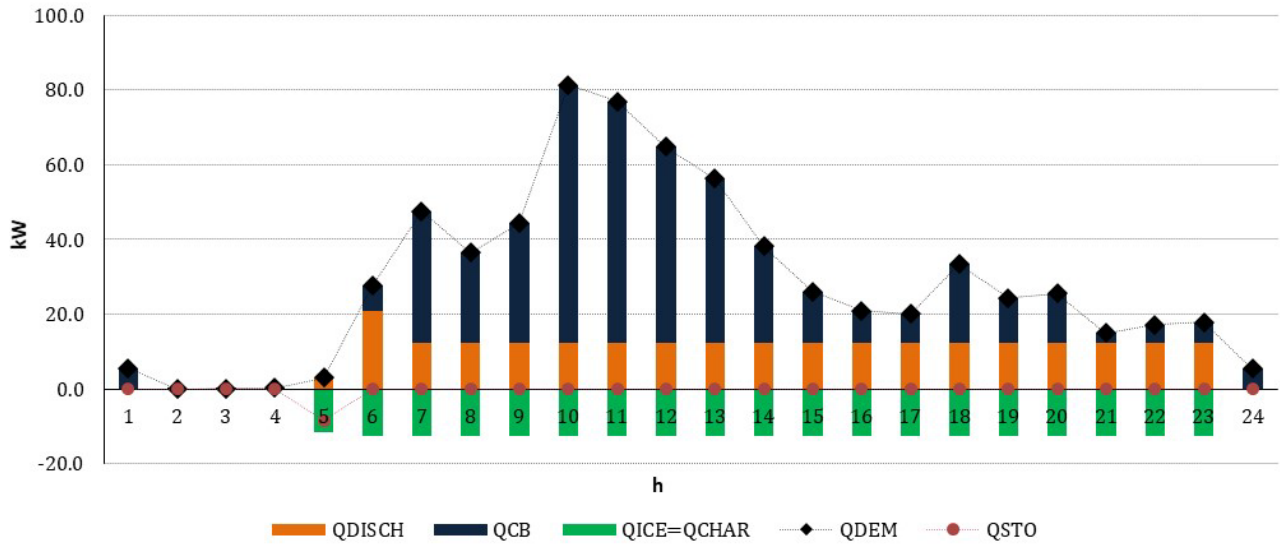
Fig. 18. Thermal balance of the maximum demand representative-day for Configuration 3
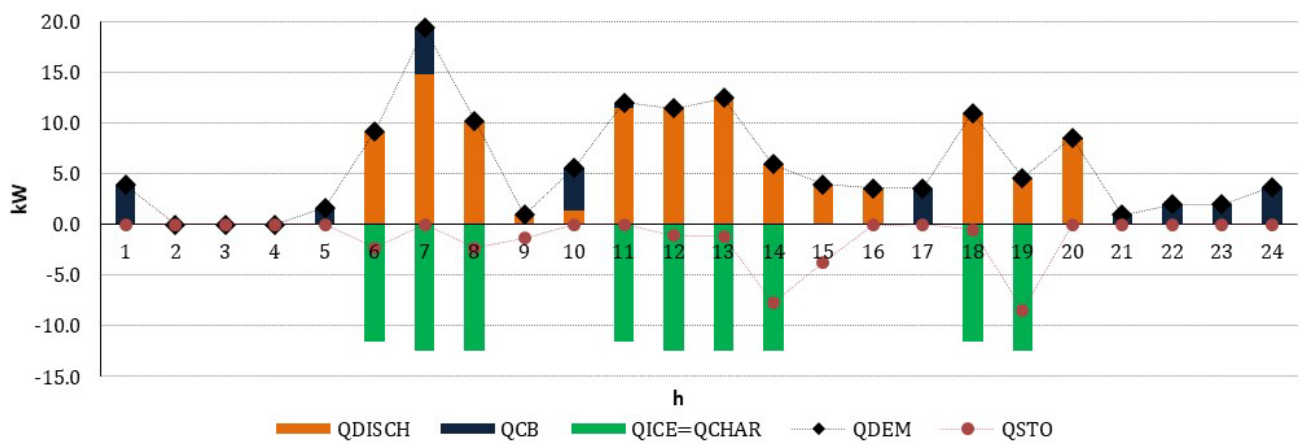

Fig. 19. Thermal balance of the minimum demand representative-day for Configuration 3

Once the optimal integration of the TES is determined, the influence of the TES capacity on the final results is approached. This analysis is applied to Configuration 3, which has been proved to be the optimal.

As can be observed in Fig. 20, the nominal thermal power of the auxiliary boiler diminishes as the volume of the TES increases, although the rate of decrease is not constant. When the volume of the tank increases over the optimal value, the slope of the curve softens and the variation of the boiler capacity is not so significant.
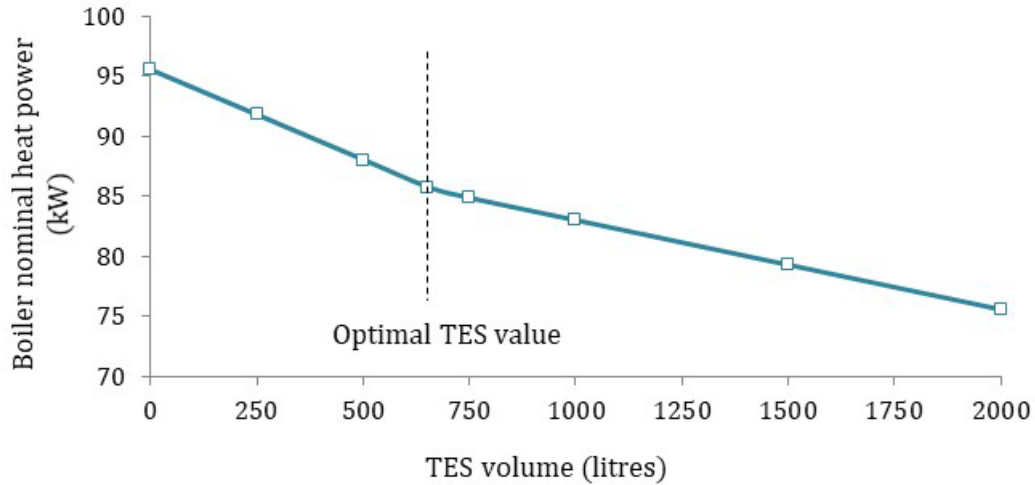
27

Fig. 20. Influence of TES volume in the variation of the boiler nominal power

On the other hand, in Fig. 21, the way useful heat provided by the TES varies in relation to its capacity is depicted. As can appreciated, there is an optimal size of the TES over which the useful heat (or covered demand) is kept virtually constant. Likewise, useful heat is related to the operation hours of the engine. As shown in Fig. 22, for values greater than the optimal TES volume, the number of operation hours of the ICE is kept virtually constant; meanwhile, for volumes below this value, the number of operation hours diminishes substantially. On the contrary, the number of start-ups of the ICE gets lower as the volume of the TES increases, with no significant variations in the slope of the curve in the optimal volume point.
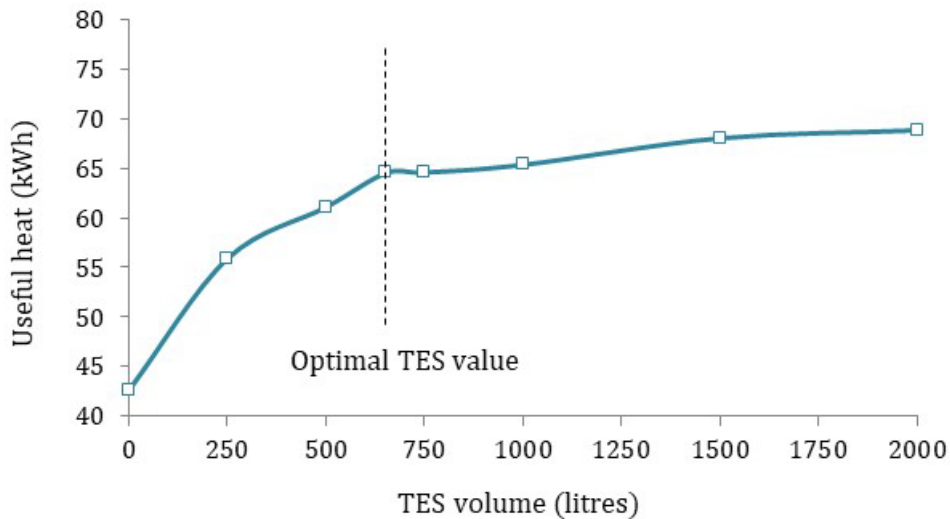

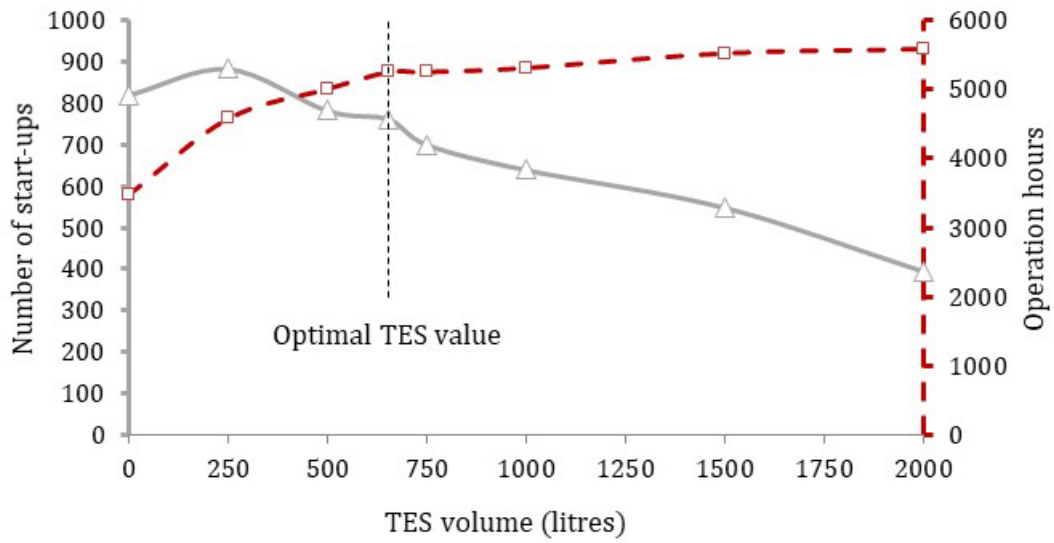**Fig. 21. Relation between useful power supplied by TES and its volume**

Fig. 22. Relation between number of start-ups/micro-CHP operation hours and TES volume
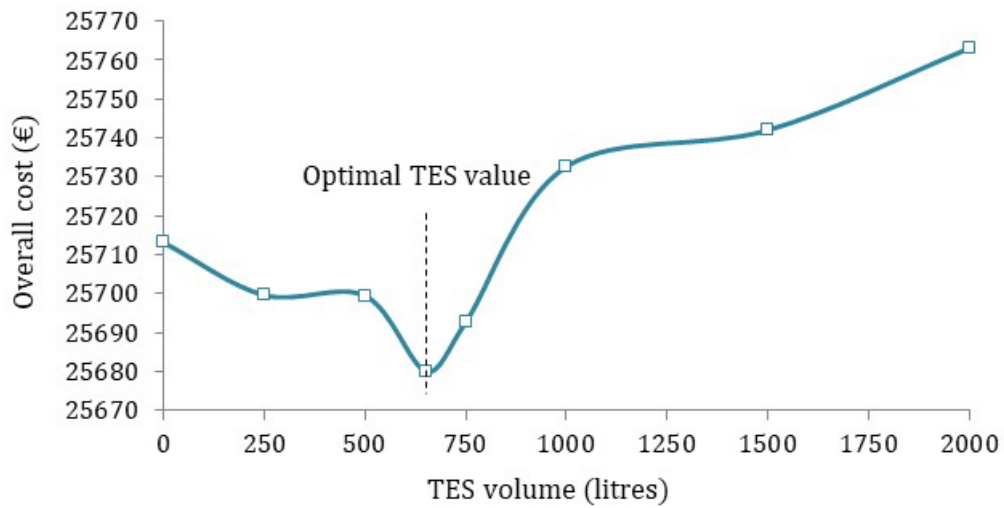

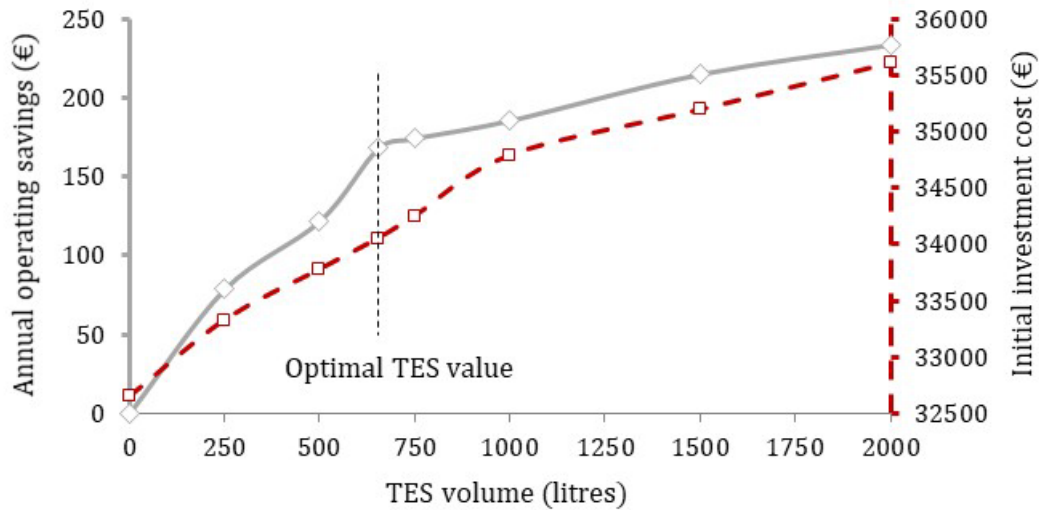**Fig. 23. Variation of global cost with TES capacity**

Fig. 24. Variation of operation cost savings and initial investment respect to the TES volume

Attending to the economics of the plant, since the accumulation volume of the TES system has been optimized attending to an economic criterion (Fig. 23), the annual global cost of the plant is at a minimum for this storage capacity.

If the investment cost and the savings attributed to the operational cost are distinguished –calculated with respect to the configuration without storage–, it can be appreciated that the investment cost increases gradually without changing the slope of the curve in the optimal value of the TES (Fig. 24). The variation in the slope of the total investment mainly depends on the investment cost of the TES, since the investment cost of the boiler is considered to change linearly with its nominal power. Regarding the saving in operational costs, it is clear that the slope of the curve changes suddenly when the optimal volume point is reached, decreasing when this value is exceeded. Thus, savings increase lightly and a greater investment in TES does not report any benefit. This optimal cost is justified by a lower rise in the slope of the useful heat once the optimal volume point is exceeded, which involves a decrease in the slope of the operational cost savings.
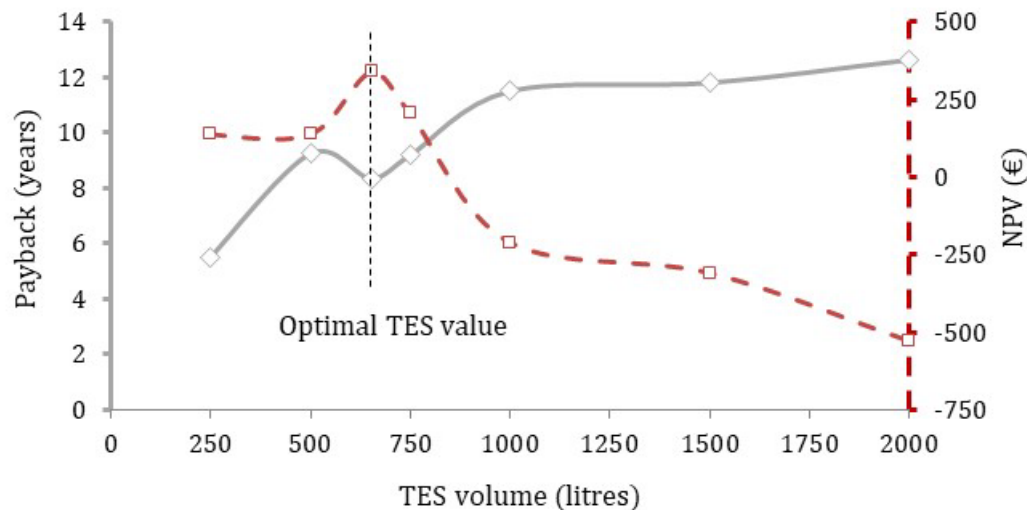

Fig. 25. Variation in payback and NPV respect to the TES volume

Due to the fact that the provided useful heat does not change considerably when the volume is greater than the optimal one, the curves of the PES, avoided emissions, and the REE all increase sharply up to this point and are maintained constant later, as shown in Fig. 26 and Fig. 27.
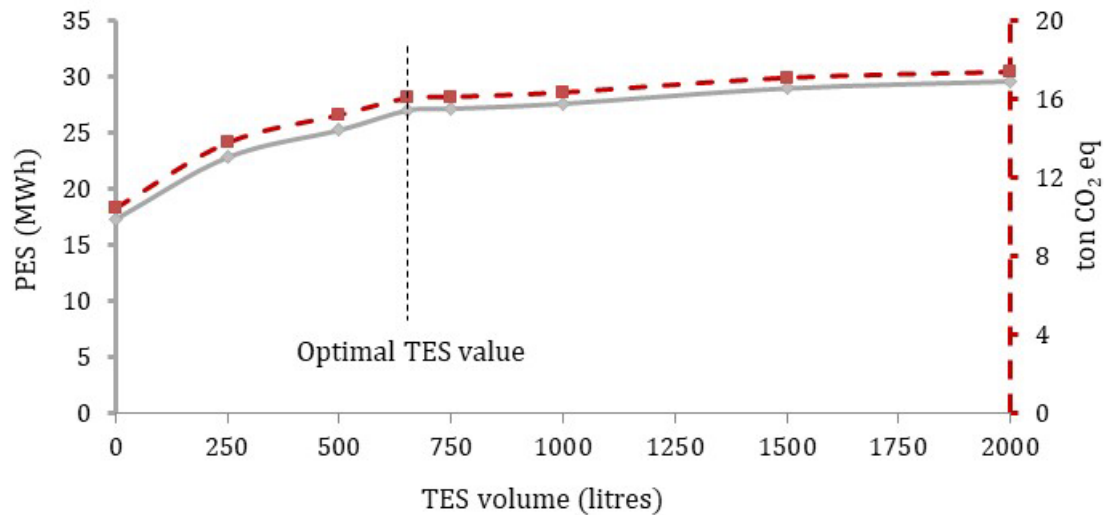
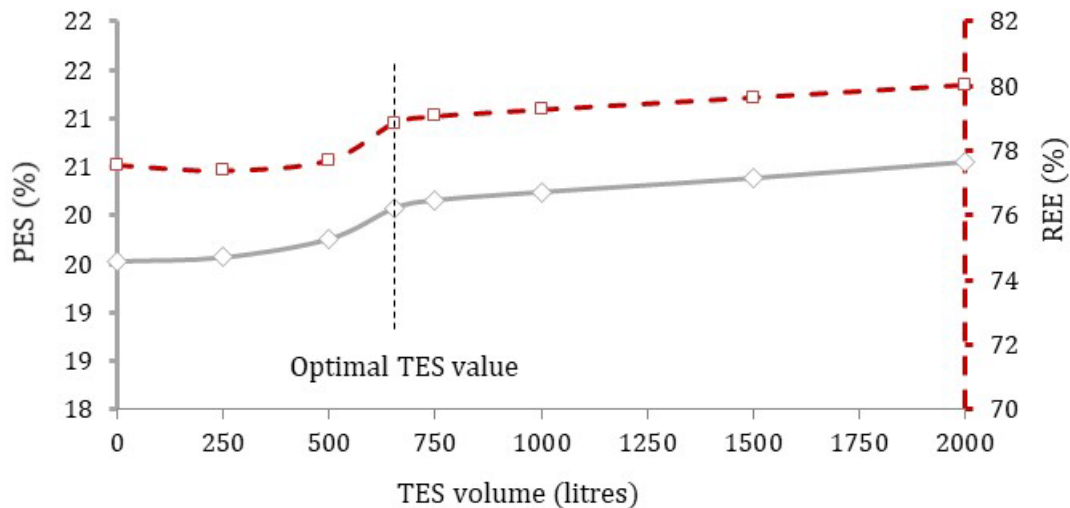Fig. 26. Variation in PES and avoided emissions respect to the TES volume

Fig. 27. Variation in PES and REE respect to the TES volume

All results obtained from the analysis lead to the conclusion that, if correctly sized, the TES is able to provide substantial thermodynamic, economic and environmental advantages.

4.1. Sensitivity analysis

Due to the influence of both the electricity and natural gas market prices in the optimal operation, a sensitivity analysis is carried out for Configuration 3. To do so, variations of ±30% are applied to current market prices and then the sizing and behaviour of the plant are analysed.

As shown in Table 2, the operation of generation devices varies significantly with the c_E/c_F ratio. It can be seen that when c_E/c_F increases, the number of hours that the micro-CHP unit operates and its contribution to DHW are greater. Furthermore, there is a value of this ratio for which the operation of the micro-CHP unit is not profitable compared to separate production. This is the case of values lower than or equal to 1.67, where the micro-CHP unit operates to meet the minimum DHW contribution. If this constraint was removed from the model, the micro-CHP unit would not operate, no TES would be installed, and the micro-CHP installation would not be economically viable; in which case the installation of renewable technologies would be necessary to supply the DHW demand required by the normative.

In the case of the greatest value of c_E/c_F, the micro-CHP unit operates to maximize the electricity production, increasing the thermal losses in the tank during the summer period and reducing the useful heat and, consequently, the REE and PES.

Regarding the design, there is no modification in the sizing of the boiler or the TES. As the capacity of the micro-CHP unit has previously been defined and the minimum contribution to DHW has to be met, sizing depends on the configuration of the plant and the peak demand. This is due to the fact that the peak demand occurs in winter, where both DHW and heating demands are high. Therefore, the micro-CHP unit can operate continuously, thus reducing the losses from start-up and storage.

Table 2. Sensitivity to changes in market prices

	c_E -30%			c_E 0%			c_E +30%		
	c_F -30%	c_F 0%	c_F +30%	c_F -30%	c_F 0%	c_F +30%	c_F -30%	c_F 0%	c_F +30%
c_E/c_F	2.17	1.52	1.17	3.10	2.17	1.67	4.03	2.82	2.17
E_{ICE} (MWh)	19.7	4.8	3.3	29.6	28.3	4.9	34.7	29.4	28.0
$Q_{ICE,U}$ (MWh)	44.7	7.9	5.8	66.9	64.6	7.9	70.1	66.7	63.8
F_{ICE} (MWh)	73.9	18.1	12.6	112.6	107.7	18.4	131.4	112.0	106.4
$Q_{CB,NOM}$ (kW)	85.7	85.7	85.7	85.7	85.7	85.7	85.7	85.7	85.7
F_{CB} (MWh)	80.0	114.4	117.8	57.3	59.7	114.4	54.1	57.5	60.4
V_{TES} (litres)	653	653	653	653	653	653	653	653	653
Operation hours	3606	885	616	5495	5252	897	6410	5465	5190
Contribution to DHW (%)	52.5	30.3	30.5	86.5	82.8	30.9	91.2	86.4	81.9
Efficiency of the plant (%)	94.8	97.7	99.2	91.2	91.9	97.5	86.2	91.3	92.0
$C_{O\&M}$ (€)	16025	18362	20576	19640	22411	25167	23164	26147	29048
C_{TOT} (€)	19294	21632	23845	22909	25680	28436	26433	29416	32318
PES (%)	20.8	7.0	8.7	19.6	20.1	6.1	15.2	19.7	20.2
REE (%)	81.0	51.6	53.7	77.3	78.9	50.6	64.7	77.7	79.1
CO_2 avoided (ton CO_{2eq})	11.3	1.9	1.4	16.6	16.1	1.9	17.2	16.6	15.9

According to the results obtained, there is a minimum c_E/c_F ratio over which the operation of the micro-CHP unit would be profitable. As shown in Fig. 28, this minimum ratio is calculated by comparing the operation cost of the cogenerated products with the cost if they were produced separately (Eq. 66). $(c_E/c_F)_{min}$ depends on the efficiencies of both the micro-CHP unit and the auxiliary boiler (Eq. 67).
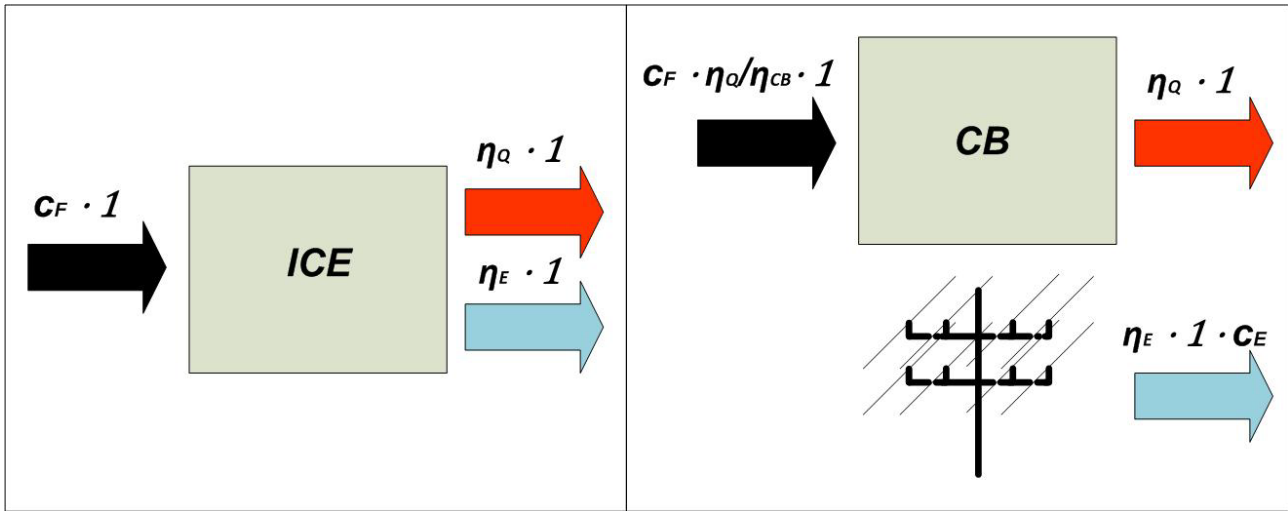
Fig. 28. Cogeneration versus separate production

$$c_F = c_F \cdot \eta_Q/\eta_{CB} + c_E \cdot \eta_E \qquad \text{Eq. 66}$$

$$(c_E/c_F)_{MIN} = \frac{(1 - \eta_Q/\eta_{CB})}{\eta_E} \qquad \text{Eq. 67}$$

The value obtained is an approximation –no storage or distribution losses have been taken into account– that can be used as reference in order to determine, in a simple way, the profitability of the micro-CHP unit operation.

5. Conclusions

This article presents the current context for the feasibility of micro-CHP installations in residential buildings. For that purpose, a MILP-based optimization model is developed for a more precise sizing and operation of the principal devices that constitute these installations: the micro-CHP unit, the auxiliary thermal generator and the TES. MILP methods require the linear modeling of non-linear constraints that characterize the optimization problem of thermal systems. As a contribution to the linear modeling of thermal systems, linear models of the behavior of storage systems and start-up periods of the micro-CHP unitare included. These considerations allow models to be obtained and subsequent results are closer to reality.

The results obtained in the optimization and comparison between the configurations, resulting from different ways of integrating TES within the thermal plant, reveal that the arrangement with intermediate storage and the possibility of simultaneous charging and discharging of the TES has greater thermodynamic, economic and environmental advantages when the TES system is correctly sized. Moreover, the configuration with thermal storage disposed in series in the return circuit presents good results, but worse than those corresponding to the parallel arrangement.

It is demonstrated that, for a given operation period, there is an optimal volume of TES, over which the useful heat supplied by the micro-CHP does not change substantially, while minimizing the operational costs of the system, as well as the generated emissions. Furthermore, primary energy savings and equivalent electric efficiency increase considerably with the volume of the TES, with low variations when the optimal volume is exceeded. Regarding economic aspects, the net present value reaches its maximum value for this optimal size of TES.

The proposed model allows the design and sizing of the devices that are part of a micro-CHP plant in the project phase to be determined, while also considering the optimal operation strategy. This information can be used by engineers and researchers to determine the viability of the plant. Even though a metaheuristic optimization with non-linear models can adjust better to the real operation, its solving-times are quite high for optimizing both sizing and operation; thus, its use is mainly focused on strategy optimization. In spite of linearization, the results obtained by means of the MILP models do not differ significantly and, in general terms, the conclusions are quite similar.

Therefore, once the optimal design and sizing have been determined by the MILP model, heuristic methods can be applied to the operation optimization of the selected devices, where the manufacturer's data can be introduced. This last analysis is beyond the scope of this paper.

Appendix A. Linearization methods

A.1 Linearization of a product of variables by means of the Big M method

In this method [54], a generic constraint is considered, where x_1 is a binary variable (or integer), x_2 is a continuous variable equal to or greater than 0, and z is the product of the variables:

$$z = x_1 \cdot x_2 \hspace{4cm} \text{Eq. 68}$$

The product of the variables $x_1 \cdot x_2$ is a nonlinear function that has to be linearized. Linearization is possible when one of the variables is integer and the other one is continuous and its value is enclosed. In this case, this problem is solved by means of the Big M Method [26], replacing the previous constraint with the following:

$$z \leq x_2 + (1 - x_1) \cdot M \hspace{3cm} \text{Eq. 69}$$

$$z \geq x_2 - (1 - x_1) \cdot M \hspace{3cm} \text{Eq. 70}$$

$$z \leq x_2 \hspace{5cm} \text{Eq. 71}$$

$$z \leq x_1 \cdot M \hspace{4.5cm} \text{Eq. 72}$$

$$z \geq 0 \hspace{5.5cm} \text{Eq. 73}$$

Thus, the obtained problem is the same as the previous one. M is a big enough number to move the constraint beyond the limits of the region inscribed by the problem. In this paper, a value of 10^7 has been chosen.

When x_1 and x_2 are binary variables, their product ($z = x_1 \cdot x_2$) is solved as follows: if x_1 is 0, x_2 will be equal to or greater than 0; whereas, if x_1 is 1, x_2 will be equal to or greater than z.

$$z \leq x_1 \; ; \; z \leq x_2 \hspace{4cm} \text{Eq. 74}$$

$$z \geq x_1 + x_2 - 1 \hspace{4cm} \text{Eq. 75}$$

A.2 Activation and deactivation of disjunctive constraints by the Big M method

Sometimes, there are constraints that cannot be satisfied at the same time, such as the task sequencing or the representation of non-convex problems. These are disjunctive constraints that cannot be met at the same time, but cannot be excluded from the problem, because it is unknown which one will be satisfied.

Supposing the following disjunctive constraints:

$$\sum_{j=1}^{n} a_{ij} \cdot x_j \leq b_i \hspace{4cm} \text{Eq. 76}$$

$$\sum_{j=1}^{n} c_{ij} \cdot x_j \leq d_i \hspace{4cm} \text{Eq. 77}$$

In order to determine which constraint is met, a binary variable δ and the constant M (M = 10^7) are used.

$$\sum_{j=1}^{n} a_{ij} \cdot x_j \leq b_i + M \cdot (1 - \delta) \hspace{3cm} \text{Eq. 78}$$

$$\sum_{j=1}^{n} c_{ij} \cdot x_j \leq d_i + M \cdot \delta$$

Eq. 79

Thus, when δ is 1 the first constraint is met and the second one is displaced from the problem, due to the value of the constant M. In contrast, when δ is 0, the second constraint is met and the first one is displaced.

A.3 Linear approximation of non-linear functions through line segments

This method is based on fitting non-linear curves through the approximation to line segments, obtaining a set of linear constraints that represent the curve. The set of pairs (z_k, $f(z_k)$) to be selected (being k=1…n) depends on the function, the linear approximation being better when the number of intervals increases.

A function $y=f(z)$ is divided into as many continuous variables as intervals:

$$z = \sum_{k=1}^{n-1} x_k$$

Eq. 80

Each variable x_k is bounded in an interval (z_k, z_{k+1}), only one of them being positive. For that, the end points of each interval are multiplied by a binary auxiliary variable, λ. Only one of these binary variables has unit value, determining the segment where the function is located.

$$z_1 \cdot \lambda_1 \leq x_1 \leq z_2 \cdot \lambda_1$$

$$z_2 \cdot \lambda_2 \leq x_2 \leq z_3 \cdot \lambda_2$$

…

$$z_{n-1} \cdot \lambda_{n-1} \leq x_{z-1} \leq z_n \cdot \lambda_{n-1}$$

Eq. 81

$$\sum_{k=1}^{n-1} \lambda_k = 1$$

Eq. 82

In order to model the y variable, the functions of segments obtained with the linear approximation are summed. For the segment (z_s, z_{s+1}), the straight line which approximates the non-linear function must pass through the points ($z_s, f(z_s)$, $z_{s+1}, f(z_{s+1})$):

$$y = f(z_s) + \frac{f(z_{s+1}) - f(z_s)}{z_{s+1} - z_s} \cdot (z - z_s)$$

Eq. 83

This can also be expressed as:

$$y = \frac{f(z_{s+1}) - f(z_s)}{z_{s+1} - z_s} \cdot z + f(z_s) - \frac{f(z_{s+1}) - f(z_s)}{z_{s+1} - z_s} \cdot z_s$$

Eq. 84

The value of the variable y is the sum of the functions in every segment, taking into account the fact that the variable z is only active for one of them.

$$y = \sum_{s=1}^{n-1} \left(\frac{f(z_{s+1}) - f(z_s)}{z_{s+1} - z_s} \right) \cdot x_s + \sum_{s=1}^{n-1} \left(f(z_s) - \frac{f(z_{s+1}) - f(z_s)}{z_{s+1} - z_s} \right) \cdot \lambda_s$$

Eq. 85

Appendix B. Technical and economic data of technologies

B.1 Condensing boilers

According to [55], the efficiency curves of natural gas condensing boilers are fitted by a polynomial equation which depends on the water return temperature and the load factor.

$$\eta_{CB} = A_1 \cdot T_r + A_2 \cdot T_r^2 + A_3 \cdot T_r^3 + A_4 \cdot T_r^4 + A_5 \cdot PL + A_6 \cdot T_r \cdot PL + A_7 \cdot T_r^2 \cdot PL + A_8 \quad \text{Eq. 86}$$

where η is the boiler efficiency between 0 and 100% referred to HHV, T_r is the return temperature in °C and PL is the load factor between 0 and 1.

The polynomial coefficients are shown in Table 3.

Table 3. Polynomial coefficients for condensing boilers [47]

COEFFICIENTS	
A1	8.663
A2	-0.2866
A3	0.003865
A4	$-1.8676 \cdot E\text{-}5$
A5	-11.102
A6	0.2822
A7	-0.00177
A8	7.626

Considering a temperature range of 80/60°C, with a constant return temperature, T_r, of 60°C, the efficiency of the condensing boilers is expressed as the following linear function:

$$\eta_{CB,HHV}(h) = 88.445 - 0.5420 \cdot PL(h) \qquad \text{Eq. 87}$$

This efficiency can also be referred to the LHV. For that, an LHV/HHV conversion factor of 0.901 is taken into account:

$$\eta_{CB,LHV}(h) = \frac{(88.445 - 0.5420 \cdot PL(h))}{0.901} \qquad \text{Eq. 88}$$

Economic data

In Fig. 29, the relation between the investment cost of natural gas condensing boilers and their nominal thermal power is shown. These values have been obtained from the manufacturer's catalogues [56, 57], where investment and installation costs of the device are considered. As can be seen, the group of data points has a lineal trend.

From the same data source, the annual maintenance cost of this type of boilers is calculated, which comes up to approximately 9.5% of the initial investment.
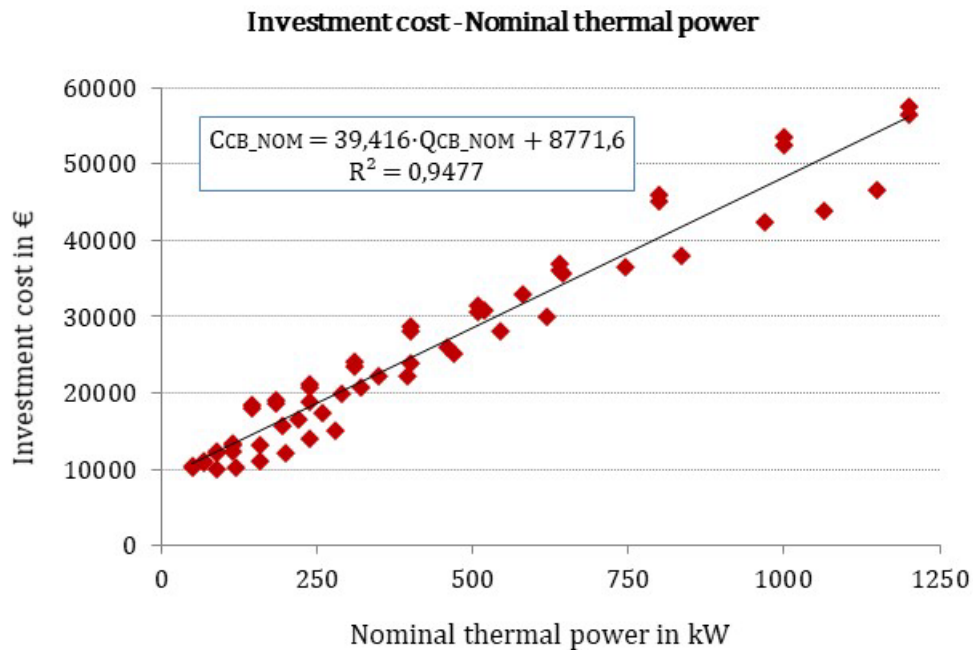
Investment cost - Nominal thermal power

$$C_{CB\_NOM} = 39{,}416 \cdot Q_{CB\_NOM} + 8771{,}6$$
$$R^2 = 0{,}9477$$

Fig. 29. Relation between investment cost and the nominal power of condensing boilers

B.2 Thermal Energy Storage

In this section, the heat losses of the TES are calculated according to the procedure developed in the technical guide "Design and calculation of the thermal insulation of pipes, appliances and equipment", developed by the Spanish Institute for Energy Saving and Diversification [58].

The Spanish Regulation for Thermal Installations in Buildings, in the document IT 1.2.4.2 [59], establishes that the thermal insulation thickness of pipes and accessories is determined depending on the diameter, fluid temperature and device location (inside or outside the building).

In the calculation, the inside and metal-wall resistances are considered to be negligible in comparison with the outside and thermal insulation resistances. The overall thermal resistance of the TES is calculated considering a thermal conductivity of $0.04 \text{W}/(\text{m} \cdot \text{K})$ for the insulation and a heat transfer coefficient of $9 \text{W}/(\text{m}^2 \cdot \text{K})$ on the outside surface [60]. For a maximum fluid temperature between 60 and 100 °C, the minimum thickness of thermal insulation required is 40 mm, provided that pipes or devices have an external diameter greater than 140 mm.

According to these criteria, in Fig. 30, the hourly TES losses for different volumes and diameter-to-height ratios are shown. These values are calculated as a percentage with respect to the heat stored at the end of the previous hour, considering a storage temperature of 70°C and an air temperature for the boiler room of 20 °C.
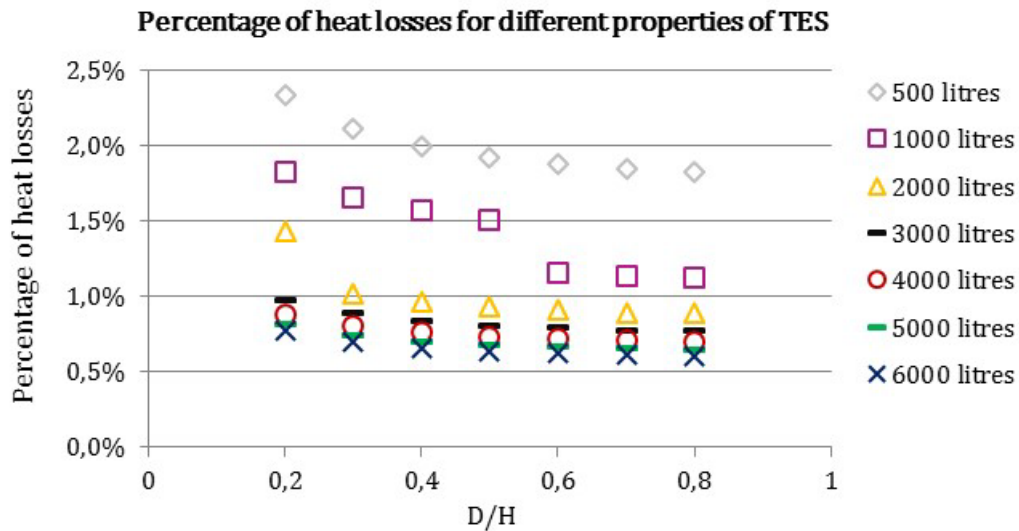
Fig. 30. Hourly thermal losses estimation for thermal storage system

Economic data

The investment cost of TES systems varies with the storage volume according to a potential function, as shown in Fig. 32.
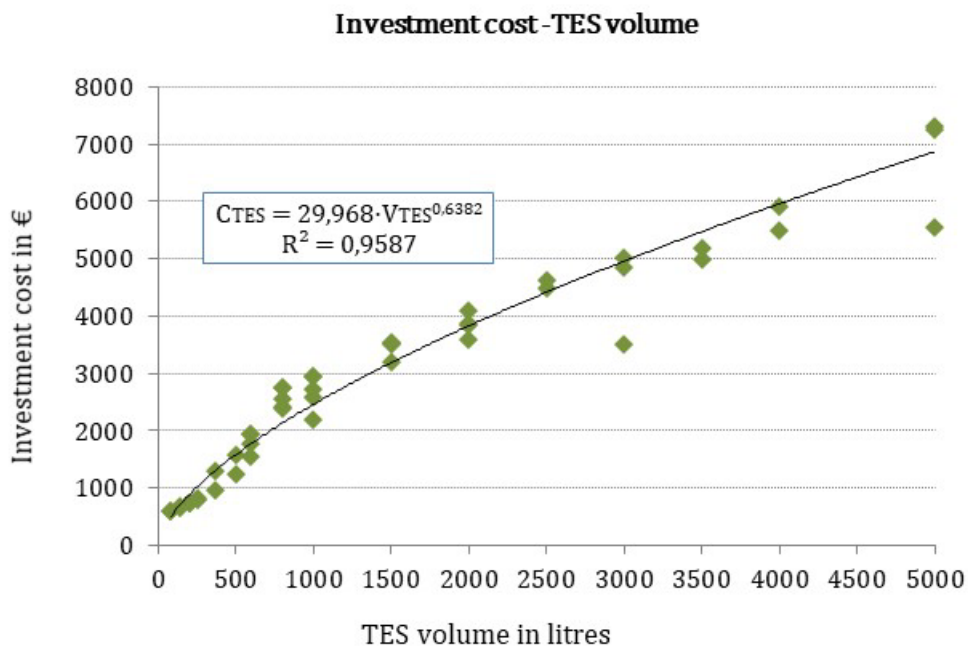

Fig. 31. Relation between the investment cost and the TES volume (Data: ITeC, CYPE [56, 57])

This function has been approximated to a linear function through line segments. In this linearization, the volume (x) is divided into different segments, where an $ax + b$ type expression is obtained. Coefficients a and b for each segment are those shown in Table 4.

Table 4. Coefficients for linear approximation of "investment cost-volume" curve

Volume (l)	a	b
0-500	3.1635	0
500-1000	1.7601	701.69
1000-5000	1.1036	1358.3

The annual maintenance cost of TES is about 2.1% of the investment cost [57].

Acknowledgements

References

[1] E. Directive, Directive 2004/8/EC of the European Parliament and of the Council of 11 February 2004 on the promotion of cogeneration based on a useful heat demand in the internal energy market and amending Directive 92/42/EEC, Official Journal of the European Union (2004) 50-60.

[2] A. Bischi, L. Taccari, E. Martelli, E. Amaldi, G. Manzolini, P. Silva, S. Campanari, E. Macchi, A detailed MILP optimization model for combined cooling, heat and power system operation planning, Energy. 74 (2014) 12-26.

[3] J.F. Bard, Short-term scheduling of thermal-electric generators using Lagrangian relaxation, Oper. Res. 36 (1988) 756-766.

[4] X.Q. Kong, R.Z. Wang, X.H. Huang, Energy optimization model for a CCHP system with available gas turbines, Appl. Therm. Eng. 25 (2005) 377-391.

[5] A. Frangioni, C. Gentile, F. Lacalandra, Tighter approximated MILP formulations for unit commitment problems, Power Systems, IEEE Transactions on. 24 (2009) 105-113.

[6] T. Li, M. Shahidehpour, Price-based unit commitment: a case of Lagrangian relaxation versus mixed integer programming, Power Systems, IEEE Transactions on. 20 (2005) 2015-2025.

[7] E. Cardona, A. Piacentino, F. Cardona, Matching economical, energetic and environmental benefits: An analysis for hybrid CHCP-heat pump systems, Energy Conversion and Management. 47 (2006) 3530-3542.

[8] G.G. Dimopoulos, A.V. Kougioufas, C.A. Frangopoulos, Synthesis, design and operation optimization of a marine energy system, Energy. 33 (2008) 180-188.

[9] A. Costa, A. Fichera, A mixed-integer linear programming (MILP) model for the evaluation of CHP system in the context of hospital structures, Appl. Therm. Eng. 71 (2014) 921-929.

[10] M.A. Lozano, J.C. Ramos, L.M. Serra, Cost optimization of the design of CHCP (combined heat, cooling and power) systems under legal constraints, Energy. 35 (2010) 794-805.

[11] S. Oh, H. Lee, J. Jung, H. Kwak, Optimal planning and economic evaluation of cogeneration system, Energy. 32 (2007) 760-771.

[12] A. Piacentino, F. Cardona, EABOT – Energetic analysis as a basis for robust optimization of trigeneration systems by linear programming, Energy Conversion and Management. 49 (2008) 3006-3016.

[13] J.C. Ramos, Optimización del diseño y operación de sistemas de cogeneración para el sector residencial comercial. Optimizing the design and operation of cogeneration systems for commercial residential sector, Universidad de Zaragoza (2012).

[14] Basic Guide. Microcogeneration., Energy Foundation of the Community of Madrid (2012).

[15] K.R. Voorspools, W.D. D'haeseleer, Reinventing hot water?: Towards optimal sizing and management of cogeneration: A case study for Belgium, Appl. Therm. Eng. 26 (2006) 1972-1981.

[16] A. Bischi, E. Pérez-Iribarren, S. Campanari, G. Manzolini, E. Martelli, P. Silva, E. Macchi, J. Sala-Lizarraga, Cogeneration systems optimization: Comparison of multi-step and mixed integer linear programming approaches, International Journal of Green Energy. 13 (2016) 781-792.

[17] S. Martínez-Lera, J. Ballester, J. Martínez-Lera, Analysis and sizing of thermal energy storage in combined heating, cooling and power plants for buildings, Appl. Energy. 106 (2013) 127-142.

[18] E.S. Barbieri, F. Melino, M. Morini, Influence of the thermal energy storage on the profitability of micro-CHP systems for residential building applications, Appl. Energy. 97 (2012) 714-722.

[19] S. Campanari, P. Manzolini, P. Silva, A multi-step optimization approach to distributed cogeneration systems with heat storage, ASME Turbo Expo,GT2008-51227 (2008).

[20] Z. Zhou, J. Zhang, P. Liu, Z. Li, M.C. Georgiadis, E.N. Pistikopoulos, A two-stage stochastic programming model for the optimal design of distributed energy systems, Appl. Energy. 103 (2013) 135-144.

[21] K.C. Kavvadias, A.P. Tosios, Z.B. Maroulis, Design of a combined heating, cooling and power system: Sizing, operation strategy selection and parametric analysis, Energy Conversion and Management. 51 (2010) 833-845.

[22] H. Ren, W. Gao, Y. Ruan, Optimal sizing for residential CHP system, Appl. Therm. Eng. 28 (2008) 514-523.

[23] G. Simader, R. Krawinkler, T. Trnka, Micro CHP systems: state-of-the-art (2006).

[24] D. Steen, M. Stadler, G. Cardoso, M. Groissböck, N. DeForest, C. Marnay, Modeling of thermal storage systems in MILP distributed energy resource models, Appl. Energy. 137 (2015) 782-792.

[25] A.J. Mason, I. Dunning, OpenSolver: Open Source Optimisation for Excel, Proceedings of the 45th Annual Conference of the ORSNZ (2010).

[26] M. Soleimani-damaneh, Modified big-M method to recognize the infeasibility of linear programming models, Knowledge-Based Systems. 21 (2008) 377-382.

[27] B. Bakhtiari, S. Bedard, Retrofitting heat exchanger networks using a modified network pinch approach, Appl. Therm. Eng. 51 (2013) 973-979.

[28] D. Steen, O. Carlson, Effects of network tariffs on residential distribution systems and price-responsive customers under hourly electricity pricing, IEEE Transactions on Smart Grid. 7 (2015) 617-626.

[29] Á Campos-Celador, E. Pérez-Iribarren, J.M. Sala, L.A. del Portillo-Valdés, Thermoeconomic analysis of a micro-CHP installation in a tertiary sector building through dynamic simulation, Energy. 45 (2012) 228-236.

[30] R. Yokoyama, Y. Hasegawa, K. Ito, A MILP decomposition approach to large scale optimization in structural design of energy supply systems, Energy Conversion and Management. 43 (2002) 771-790.

[31] M. Casisi, P. Pinamonti, M. Reini, Optimal lay-out and operation of combined heat & power (CHP) distributed generation systems, Energy. 34 (2009) 2175-2183.

[32] J. Ortiga, J.C. Bruno, A. Coronas, Selection of typical days for the characterisation of energy demand in cogeneration and trigeneration optimisation models for buildings, Energy Conversion and Management. 52 (2011) 1934-1942.

[33] G. Mavrotas, D. Diakoulaki, K. Florios, P. Georgiou, A mathematical programming framework for energy planning in services' sector buildings under uncertainty in load demand: The case of a hospital in Athens, Energy Policy. 36 (2008) 2415-2429.

[34] Z. Beihong, L. Weiding, An optimal sizing method for cogeneration plants, Energy Build. 38 (2006) 189-195.

[35] S. Yoshida, K. Ito, R. Yokoyama, Sensitivity analysis in structure optimization of energy supply systems for a hospital, Energy Conversion and Management. 48 (2007) 2836-2843.

[36] M.A. Lozano, J.C. Ramos, M. Carvalho, L.M. Serra, Structure optimization of energy supply systems in tertiary sector buildings, Energy Build. 41 (2009) 1063-1075.

[37] F. Domínguez-Muñoz, J.M. Cejudo-López, A. Carrillo-Andrés, M. Gallardo-Salazar, Selection of typical demand days for CHP optimization, Energy Build. 43 (2011) 3036-3043.

[38] F. Domínguez-Muñoz, A. Carrillo-Andrés, G. Calleja-Rodríguez, E.A. Rodríguez-García, Influencia del número de días tipo en la optimización de plantas térmicas centralizadas, CNIT (2013).

[39] S.C. Jansen, J. Terés-Zubiaga, P.G. Luscuere, The exergy approach for evaluating and developing an energy system for a social dwelling, Energy Build. 55 (2012) 693-703.

[40] IDAE, Evaluation of the potential of solar thermal air conditioning in buildings, Institute for Energy Diversification and Saving, Ministry of Industry, Tourism and Commerce, Spanish Government (2011).

[41] CTE, Spanish Technical Building Code, Basic Document HE 4: Solar Minimum Contribution for Domestic Hot Water, Ministry of Housing, Spanish Government, Madrid (in Spanish) (2013).

[42] Ministry of Health and Consumption, RD 865/2003 of 4 July, establishing the hygienic criteria for the prevention and control of legionellosis, Madrid, 2003 (in Spanish).

[43] Energy keys to domestic sector in the Basque Country: EVE 2013 (in Spanish).

[44] RITE, modifications to the new regulations on thermal installations in buildings, approved by RD 238/2013, BOE-A-2013-3905, Ministry of the Presidency, Madrid (2013).

[45] Senertec Dachs Commercial Catalogue. http://www.senertec.es/es/derdachs.html.

[46] IDAE, Factores de emisión de CO_2 y coeficientes de paso a energía primaria de diferentes fuentes de energía final consumidas en el sector edificios en España, Ministry of Industry, Tourism and Commerce (2016).

[47] E. Pérez-Iribarren, A. Campos-Celador, J. Sala-Lizarraga, L. del Portillo-Valdés, Exergoenvironmental analysis of a residential micro-CHP installation. 4 (2011) e6.

[48] IDAE. Eligibility guide of projects in charge of the JESSICA F.I.D.A.E holding fund. Madrid: Institute for Energy Diversification and Saving, Ministry of Industry, Energy and Tourism, Spanish Government; 2014 [in Spanish].

[49] European Union Regional Policy. Guide to cost benefit analysis of investment projects. 2008.

Pérez-Iribarren, E., González-Pino, I., Azkorra-Larrinaga, Z., Gómez-Arriarán, I.. Optimal design and operation of thermal energy storage systems in micro-cogeneration plants. Applied Energy, 2020, 265, 114769

[50] I. Beausoleil-Morrison, Experimental Investigation of Residential Cogeneration Devices and Calibration of Annex 42 Models, Annex 42 of the International Energy Agency Energy Conservation in Buildings and Community Systems Programme (2007).

[51] E.E. Directive, Directive 2012/27/EU of the European Parliament and of the Council of 25 October 2012 on energy efficiency, amending Directives 2009/125/EC and 2010/30/EU and repealing Directives 2004/8/EC and 2006/32, Official Journal, L. 315 (2012) 1-56.

[52] Commission Decision 2007/74/EC. Commission Decision of 21 December 2006 establishing harmonised efficiency reference values for separate production of electricity and heat in application of Directive 2004/8/EC of the European Parliament and of the Council.

[53] Ministry of Industry, Tourism and Commerce, RD 661/2007, of May 11th, on the promotion of cogeneration (BOE n.114), Madrid (2007).

[54] W.L. Winston, J.B. Goldberg, Operations research: applications and algorithms, Duxbury press Boston, 2004.

[55] J. Cockroft, A. Samuel, P. Tuohy, Development of a Methodology for the Evaluation of Domestic Heating Controls. Phase 2 of a DEFRA Market Transformation Programme project, carried out under contract to BRE Environment. Final Report. (2007).

[56] Instituto de Tecnología de la Construcción ITeC, http://itec.es/nouBedec.e/.

[57] CYPE INGENIEROS, Software para Arquitectura, Ingeniería y Construcción, http://www.generadordeprecios.info/
 (2015).

[58] IDAE, Technical Guide Nº3. Design and calculation of the thermal insulation of pipes, appliances and equipment, Institute for Energy Diversification and Saving, Ministry of Industry, Tourism and Commerce, Spanish Government, Madrid (2007).

[59] RITE, the new regulations on thermal installations in buildings , approved by RD 1027/2007, BOE 29.08.07, Ministry of the Presidency, Madrid (2007).

[60] L. Jutglar, A.L. Miranda, M. Villarrubia, Manual de Calefacción Ferroli (2011).